

Review

Development of Optical Differential Sensing Based on Nanomaterials for Biological Analysis

Lele Wang, Yanli Wen *, Lanying Li, Xue Yang, Wen Li, Meixia Cao, Qing Tao, Xiaoguang Sun and Gang Liu *

Key Laboratory of Bioanalysis and Metrology for State Market Regulation, Shanghai Institute of Measurement and Testing Technology, 1500 Zhang Heng Road, Shanghai 201203, China; wangll@simt.com.cn (L.W.); lily@simt.com.cn (L.L.); yangxue@simt.com.cn (X.Y.); liw@simt.com.cn (W.L.); caomx@simt.com.cn (M.C.); taoq@simt.com.cn (Q.T.); sunxg@simt.com.cn (X.S.)

* Correspondence: wenyli@simt.com.cn (Y.W.); liug@simt.com.cn (G.L.)

Abstract: The discrimination and recognition of biological targets, such as proteins, cells, and bacteria, are of utmost importance in various fields of biological research and production. These include areas like biological medicine, clinical diagnosis, and microbiology analysis. In order to efficiently and cost-effectively identify a specific target from a wide range of possibilities, researchers have developed a technique called differential sensing. Unlike traditional “lock-and-key” sensors that rely on specific interactions between receptors and analytes, differential sensing makes use of cross-reactive receptors. These sensors offer less specificity but can cross-react with a wide range of analytes to produce a large amount of data. Many pattern recognition strategies have been developed and have shown promising results in identifying complex analytes. To create advanced sensor arrays for higher analysis efficiency and larger recognizing range, various nanomaterials have been utilized as sensing probes. These nanomaterials possess distinct molecular affinities, optical/electrical properties, and biological compatibility, and are conveniently functionalized. In this review, our focus is on recently reported optical sensor arrays that utilize nanomaterials to discriminate bioanalytes, including proteins, cells, and bacteria.

Keywords: pattern recognition; nanomaterials; gold nanoparticle; graphene oxide; quantum dot



Citation: Wang, L.; Wen, Y.; Li, L.; Yang, X.; Li, W.; Cao, M.; Tao, Q.; Sun, X.; Liu, G. Development of Optical Differential Sensing Based on Nanomaterials for Biological Analysis. *Biosensors* **2024**, *14*, 170. <https://doi.org/10.3390/bios14040170>

Received: 28 February 2024

Revised: 25 March 2024

Accepted: 29 March 2024

Published: 31 March 2024



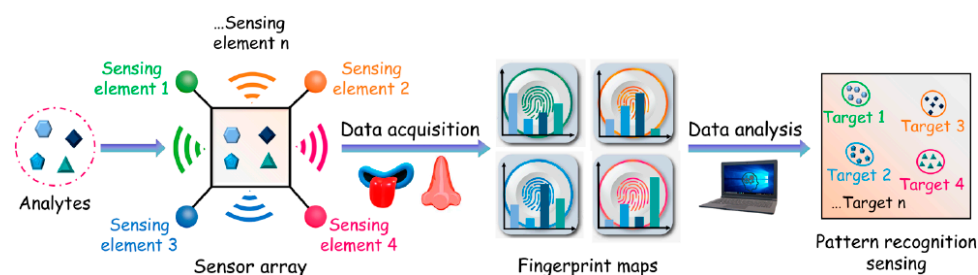
Copyright: © 2024 by the authors. Licensee MDPI, Basel, Switzerland. This article is an open access article distributed under the terms and conditions of the Creative Commons Attribution (CC BY) license (<https://creativecommons.org/licenses/by/4.0/>).

1. Introduction

In recent decades, natural/artificial specific receptors have been studied for the analysis of particular analytes based on the lock-and-key principle in many critical fields, including food safety [1–11], environmental monitoring [12–17], and medical diagnosis [18–31]. However, the production of highly specific receptors remains a challenge for a large range of analysis targets, especially when facing complex biological samples containing proteins, microorganisms, and cells.

Recently, pattern recognition has been intensively studied, also known as differential sensing or “artificial noses/tongues” [32–37]. Different from traditional molecular recognition based on one specific receptor, differential sensing was constructed on a receptor library of low-specific recognizing elements, each of which would respond to a certain target to different degrees [38–40]. By collecting the response signals, we can establish a fingerprint toward characteristic patterns for the individual analytes or complex mixtures. To perform differential sensing, a sensor array was constructed as the central component. Through array analysis, data from various sensing units could be gathered concurrently and subsequently scrutinized to facilitate target detection and recognition (Scheme 1). The number of channels within the array is a crucial factor influencing the discrimination capacity of the differential sensor. An illustrious example highlighting this principle is the olfactory system of a dog, which possesses approximately 4 billion olfactory receptor cells, an astonishing 45 times more than that of a human. The signals detected by these receptors

have the potential to generate even larger quantities of interconnected data groups through their intricate associations with one another.



Scheme 1. Mechanisms of Sensor Arrays for Discrimination and Identification of Analytes. Reprinted with permission from [33]. Copyright 2023 American Chemical Society.

There are two main obstacles to the development of artificial sensors: Firstly, it is difficult to construct a large-scale array to collect adequate signals compared with natural systems. Secondly, the sensitivity is usually hindered by the relatively high blank noise signal or low signal read-out, especially in biological samples. Thus, there have been increasing research demands to develop novel biosensing strategies for higher sensitivity and larger scale of sensor arrays [37]. In recent decades, nanomaterials have become a shining star in the research of a growing number of biosensor strategies [41–50]. The emergence of fast-growing nanomaterials [51], such as metal nanoparticles [48,52–56], carbon nanomaterials [44,46,57,58], and quantum dots [59–61], has opened up exciting possibilities for novel sensor platforms [62–64]. These nanomaterials possess unique electronic, magnetic, and light properties, making them highly desirable for the field of differential sensing. Table 1 displays the main characteristics of the common nanomaterials studied for optical differential sensing.

Table 1. The main characteristics of the common nanomaterials studied for optical differential sensing.

Nanomaterials	Biological Interaction	Optical Signal
AuNPs	Competitive adsorption, Au-S modification	fluorescence quenching, Colorimetric signal due to aggregation
Graphene oxide (GO)	Competitive adsorption, Modification through -COOH	fluorescence quenching
QDs	Bind nonspecifically via electrostatic interactions	Fluorescence emission with different lengths and high quantum yield

In this review, we present an overview of the applications of functional nanomaterials in optical sensor arrays, including colorimetric and fluorescence methods. These arrays can be categorized into gold nanoparticle-based sensor arrays, graphene oxide (GO)-based sensor arrays, quantum dot (QD)-based sensor arrays and other metal nanoparticle-based sensor arrays. Table 2 presents the timeline for the historical development of optical differential sensing based on nanomaterials for biological analysis. Compared to the former literature, this review aims to provide a comprehensive understanding of the advancements, challenges, and future prospects in this rapidly evolving field. We here mainly focus on three main significant advantages and contributions of nanomaterials for the development of sensor arrays: Firstly, by manipulating their physical and chemical properties as well as surface modifications, functional nanomaterials enhance signal output, sensitivity, and selectivity. Secondly, the unique properties and interaction mechanisms of functional nanomaterials enable sensor arrays to detect multiple target molecules and achieve multiparameter analysis. Additionally, functional nanomaterials allow for efficient analysis of complex samples by integrating multiple sensing mechanisms such as fluorescence resonance energy transfer and surface plasmon resonance. Thus, the integration of

functional nanomaterials into sensor arrays holds great promise in advancing the field of optical sensing, offering new avenues for exploring various detection technologies and expanding the range of potential applications.

Table 2. Development of optical differential sensing based on nanomaterials for biological analysis in different timelines.

Year	Development of Optical Differential Sensing Based on Nanomaterials for Biological Analysis
2007	Rotello's group developed a sensor array consisting of six non-covalent gold nanoparticle-fluorescent polymer conjugates for identification and quantitative differentiation of proteins [65]
2010	Rotello and co-workers developed enzyme-amplified array sensing (EAAS) with NPs to dramatically increase the sensitivity for protein identification [38]
2012	Rotello and co-workers also achieved colorimetric differentiation of proteins with catalytically active NPs used for both recognition and signal transduction/amplification [66]
2012	Rotello and co-workers also developed gold-nanoparticle green-fluorescent protein (NP-GFP)-based sensor arrays for the identification of mammalian cell types and cancer states [67]
2012	Dravid, Chou, and De developed nanoscale graphene oxide (nGO) as artificial receptors for array-based protein identification [68]
2012	Fan, Hu, and co-workers employed the combination of fluorescently labeled adaptive "ensemble aptamers" (ENSaptamers) and nGOs for high-precision identification of a wide range of bioanalytes, including proteins, cells, and bacteria [69]
2014	Ouyang and co-workers have synthesized novel blue-emitting ColAu NCs and Mac-Au NCs for discriminating proteins [70]
2014	Qu and Ren utilized a sensing array composed of seven luminescent nanodots, combined with graphene oxide, for protein recognition [71]
2015	He and Chang constructed an array-based protein discrimination system by using eight Au NDs as efficient protein receptors and competent signal transducers [72]
2016	Zhang and Tang develop a multicolor quantum dot (QD)-based multichannel sensing platform for rapid identification of multiple proteins [73]
2017	Shi and Wu employed a colorimetric sensor array consisting of four gold nanoparticles (AuNPs) with diverse surface properties for the rapid identification of microorganisms [74]
2018	Pu, Ren and Qu developed a sensitive and effective method for pattern recognition of proteins using nanozyme (g-C ₃ N ₄) as a receptor [75]
2022	Li and Han utilized five fluorescent positively charged polymers (P1–P5) and negatively charged graphene oxide (GO) for differentiating between different proteins [76]
2022	Huang, Han and Li utilized three modified polyethyleneimine and negatively charged graphene oxide for differentiating different bacteria [77]
2023	Tian and Wu utilized silver nanoparticles for differentiating proteins in various osmolyte solutions [78]
2024	Yang employed DBCO-UCNPs for the differentiation of different pathogens in terms of phenotyping classification and antibiotic resistance identification [34]

2. Pattern Recognition Methods for Differential Sensing

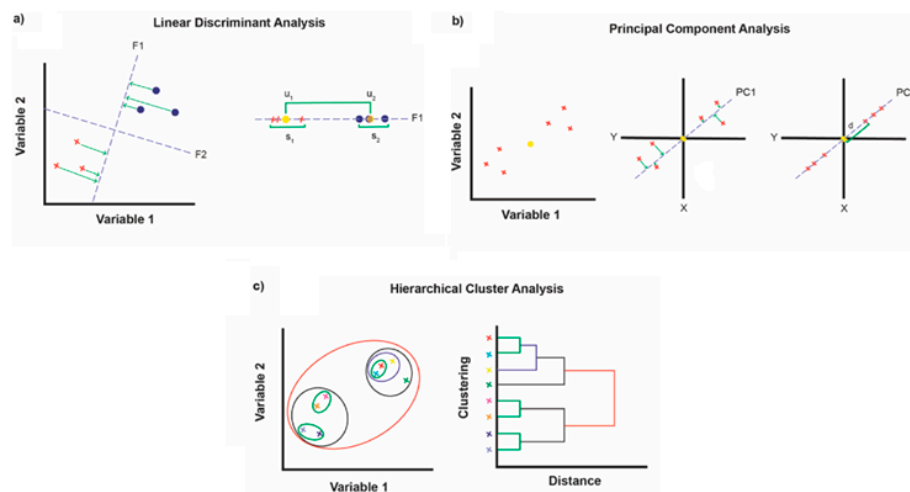
Optical signals produced by the differential sensing array were analyzed by using pattern recognition methods such as linear discriminant analysis (LDA) [79], principal component analysis (PCA) [80], and hierarchical clustering analysis (HCA) [81]. A schematic representation of the above methods is shown in Scheme 2.

Linear discriminant analysis is a supervised pattern recognition method that can be used for both dimensionality reduction and classification [82]. The means and covariance matrices of the training data set are used to establish the discriminant functions. Once the discriminant functions are built, a prediction data set is tested by the discriminant functions to validate the classification accuracy. In order to ensure classification accuracy,

the prediction data set should be different from the training data set; otherwise, LDA may produce optimistic results.

Principal component analysis (PCA) is an unsupervised method for dimensionality reduction of multivariate data. It can compress a multi-dimensional data set into a lower dimensional space and rank the new dimensions according to their importance. Often, a successful PCA may produce two or three principal components, which are convenient for producing score plots for the data set [83]. It is important to note that PCA is more suitable for the analysis of linear data; however, it is possible to fail the classification of nonlinear data.

Similar to PCA, hierarchical clustering analysis (HCA) is an unsupervised pattern recognition method. There are three basic steps for HCA: Firstly, the multivariate distances between all samples are calculated. Afterward, clustering is performed by establishing a hierarchy of points, in which similar distant points are joined. Finally, a two-dimensional dendrogram is shown that allows the visual examination of clustering relationships of all samples [84]. Because HCA employs all the sensor array data to represent the patterns, a poor result may be produced when the data set is noisy. HCA is most suitable for qualitative analysis of relationships in data.



Scheme 2. Schematic representation of (a) the LDA method of projecting points onto a new vector $F1$ that fulfils the criteria of maximizing the ratio of between-class to within-class variance, (b) the PCA method of determining the center of the data, projecting points onto a new vector, and calculating the maximum variance and thus the best-fitting line, (c) the HCA bottom-up agglomerative approach and the resulting dendrogram illustrating the connectivity of data points. Reprinted with permission from [85]. Copyright 2021 American Chemical Society.

3. Gold Nanoparticle-Based Sensor Arrays

Gold nanoparticles (AuNPs) have been widely studied in the development of biosensors due to their unique optical and chemical properties, good biocompatibility, and easy surface functionalization [86–88]. Together with organic or biological molecules, AuNPs can produce differential response signals for target molecules [65,67,74,89–113].

3.1. Fluorescence Sensing Based on AuNPs

AuNPs are widely applied in biosensors as powerful fluorescence quenchers [114–120]. The competitive bindings between the analytes and the indicators to AuNPs lead to distinct fluorescence response fingerprints for many analytes, which could be identified by pattern recognition methods with a high degree of accuracy [121]. These AuNPs work as powerful fluorescence quenchers for fluorescence indicators, as well as the recognition elements for target analytes. The interactions between nanoparticle–indicators and nanoparticle–analytes could be tuned by modifying different groups on the surface of AuNPs.

A sensor array was developed for the differentiation of normal and cancerous cell lines, based on conjugates between three structurally related cationic AuNPs and the fluorescent polymer [90,122]. The nanoparticles quench the fluorescence of the polymer. In the presence of mammalian cells, there is competitive binding between nanoparticle-polymer complexes and cell types. The polymer was displaced with mammalian cells from the nanoparticle surface, generating a fluorescence response. Four different types of human cancer cells were discriminated by using LDA. The results showed a 100% accuracy of detection. The sensor array can also effectively differentiate isogenic cell types. Later, the same group designed a sensor array composed of AuNP-GFP complexes for discrimination between normal and metastatic cells and tissues [67]. Rather than using whole cells as the target analytes, the lysates isolated from tissues have the advantage of increased homogeneity of the test samples, which leads to reduced error in identification, increased reproducibility, and higher sensitivity. This sensing platform needed a small amount of sample (as little as 200 ng of cell- or tissue-lysed proteins).

The Rotello group synthesized two types of AuNPs, one with a cationic hydrophobic functional group and the other with a hydrophilic functional group [70] (Figure 1). Three fluorescent proteins with negative surface charge can bind to these particles through electrostatic interactions, resulting in fluorescence quenching. When exposed to bacteria biofilms, AuNP-fluorescent protein conjugates are disrupted to produce different colored fluorescence patterns. The multichannel sensor was able to completely differentiate six bacterial biofilms, including nonpathogenic and pathogenic bacteria. The performance of the sensor was further tested by the identification of biofilms in a mixed bacteria/mammalian cell in vitro wound model.

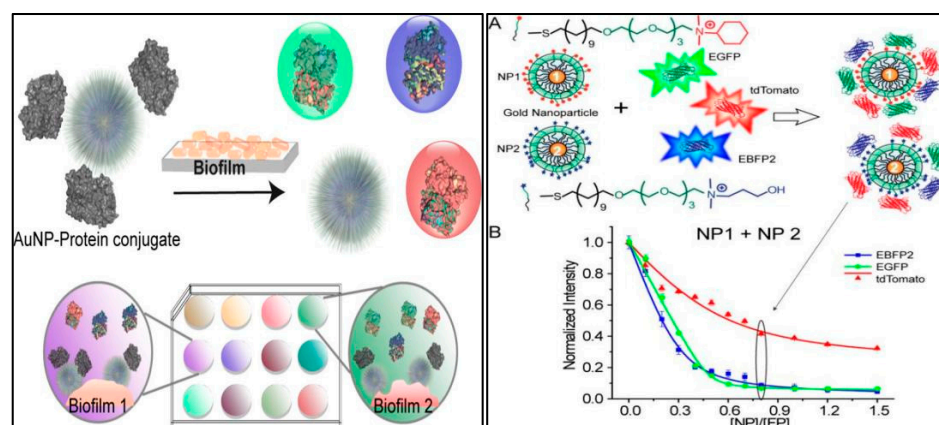


Figure 1. (Left) Schematic illustration of the multichannel sensor using AuNP-fluorescent protein conjugates that are disrupted in the presence of biofilms. (Right) The sensor composition. (A) Sensor elements and molecular structures of the functional ligands of NP1 and NP2. (B) Fluorescence titration with an equal molar mixture of NP1 and NP2. Reprinted from [70] with open access.

3.2. Colorimetric Sensing Based on AuNPs

The aggregation of AuNPs results in a visible color change from red to blue, which provides a versatile platform for colorimetric sensing of target analytes [96,123–125]. Zhang and co-workers created a colorimetric sensor array with aptamer-protected AuNPs as recognition elements [126]. The aptamer-protected AuNPs were able to resist aggregation in the presence of a high-concentration salt. Upon the addition of different target proteins, differential response patterns were obtained. This sensitive array sensing system can discriminate seven proteins with the naked eye at the 50 nM level. Similar approaches were also used for the analysis of many bioanalytes [127–129]. These sensor arrays exhibited an excellent ability to recognize proteins, bacteria, and mammalian cells.

Chen et al. constructed a DNA-AuNPs colorimetric sensor array for rapid and sensitive identification of proteins [128]. The sensor array composed of only two sensing elements could discriminate 12 proteins at the 50 nM level with the naked eye. Moreover, the proteins

in human serum and protein mixtures were well-differentiated with 100% accuracy. Huang and co-workers also exploited DNA-AuNPs nanoconjugates to differentiate cell types [129]. The cross-reactive receptors (DNA-AuNPs) are employed to bind the different cells that produce differential color changes of AuNPs. The nanoplasmonic effect of AuNPs was enhanced via seeded growth, which resulted in the effective distinction of various cell lines with dark-field microscopy or even the naked eye. The results were analyzed by LDA, which showed 100% accuracy.

Wu and Shi [28] developed a colorimetric sensor array for rapid microorganism identification. The array utilized four distinct AuNPs as sensing elements, resulting in noticeable color shifts upon interaction with microorganisms. Through LDA, 15 microorganisms were successfully differentiated based on their unique response patterns. The sensor array also demonstrated the ability to discern mixtures of microorganisms. This straightforward and expedient method provides results within 5 s, making it suitable for applications in pathogen diagnosis and environmental monitoring.

A colorimetric sensor array was developed using D-amino acid (D-AA)-modified AuNPs as probes (Au/D-AA) for bacteria fingerprinting [130]. The aggregation of AuNPs is triggered by the metabolic activity of bacteria towards D-AA, allowing differentiation of eight types of bacteria and quantitative analysis of a single bacterium. The sensor array also enables rapid colorimetric antibiotic susceptibility testing (AST) by monitoring bacterial metabolic activity toward different antibiotic treatments, which has implications for clinical applications and antibiotic stewardship (Figure 2).

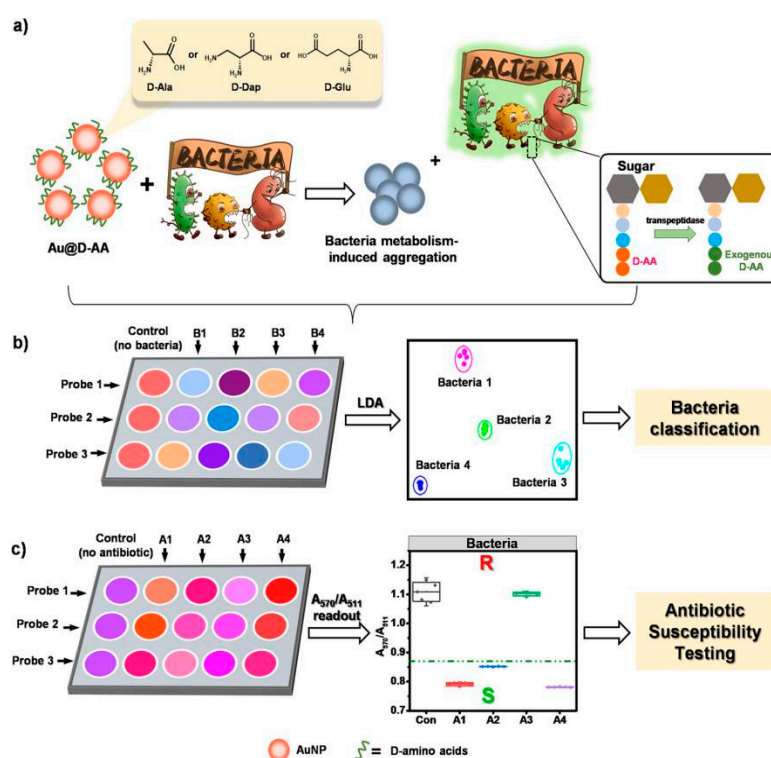


Figure 2. Principle of the Developed Assay Based on the Bacteria Metabolism-Triggered Consumption of dD-AA (a), Strategies for Multiple Bacteria Identifications through LDA (b) and AST through the Colorimetric Change of Probes after the Incubation with Bacteria and Antibiotic (c). Reprinted with permission from [130]. Copyright 2022 American Chemical Society.

Liu and co-workers presented an extensible multidimensional sensor using the conjugates of nonspecific dye-labeled DNA sequences and AuNPs as receptors [127]. The changes in the fluorescent and colorimetric signals were generated by the addition of the target proteins due to the competitive binding. The array has a strong ability to distinguish

11 protein analytes with a detection limit as low as 50 nM. Also, 10 proteins at 1.0 μM were well-identified when the proteins were spiked into the human urine sample.

3.3. Differential Sensing Based on Gold Nanoclusters (AuNCs)

More recently, AuNCs have attracted much interest in biosensing applications [131–134]. Compared with semiconductor quantum dots or other metal NDs, AuNCs possess several distinct features, such as photophysical/chemical properties, good stability, and excellent biocompatibility [135–142]. Several studies utilized AuNCs for the construction of differential sensing strategies [72,143–145]. Ouyang and co-workers designed a visual sensor array based on blue-emitting Col-AuNCs and Mac-AuNCs for the discrimination of proteins [70]. The colorimetric and fluorometric signal changes were recorded after the addition of the target proteins. Either or both proteins and protein mixtures after polyacrylamide electrophoresis were well-discriminated by LDA.

Luo's group also developed a protein sensing platform using six dual ligand functionalized AuNCs as sensing receptors [144], by functionalizing them with different amino acids. When they compared the relative fluorescence changes with the LDA method, ten proteins were successfully discriminated. Wu and co-workers [146] developed a fluorescence sensor array based on metal ion-AuNCs for the identification of proteins and bacteria. The sensor array successfully differentiated nine proteins with different concentrations and identified five different types of bacteria, demonstrating its potential for rapid and sensitive biomolecule sensing.

A pH-controlled histidine-templated AuNC (AuNCs@His) [147] was developed for a fluorescent sensor array that responds to reactive oxygen species (ROS) for distinguishing cancer cell types and their proliferation states. The sensor array exhibited excellent performance in accurately differentiating cancer cell types and their proliferation states, indicating great potential for precise cancer diagnosis (Figure 3). Li and Zhu [148] developed a multichannel sensor array for efficient identification of bacteria based on three antimicrobial agents (vancomycin, lysozyme, and bacitracin) functional AuNCs. This sensing platform successfully differentiated seven pathogenic bacteria, different concentrations of the same bacteria, and even bacterial mixtures, offering a rapid and reliable method for diagnosing urinary tract infections.

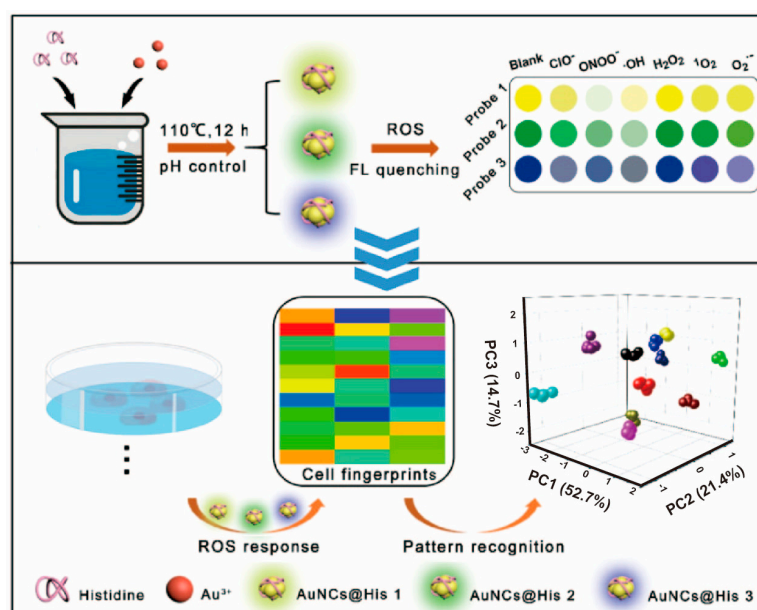


Figure 3. Schematic diagram of precise diagnosis of cancer via an ROS-responsive fluorescent sensor array based on pH-controlled multicolor histidine-templated AuNCs. Reprinted with permission from [147]. Copyright 2023 American Chemical Society.

In summary, gold nanoparticles are good candidates for the development of sensor arrays for biological analysis, and the main characteristics of the different sensor arrays are shown in Table 3.

Table 3. Summarization of Gold Nanoparticle-Based Sensor Array Construction Strategies with Different Artificial Receptors (ARs).

Nanomaterials	Strategies	Numbers of ARs	Signals	Data Analysis Methods	Analytes	LOD	Ref.
AuNPs	Competitive binding between nanoparticle-polymer complexes and cells	3	Fluorescence	LDA	Cells	n.a.	[90]
AuNPs	Competitive binding between NP-GFP complexes and cells	6	Fluorescence	LDA	Cells	5000 cells	[91]
AuNPs	Proteins displace β -Gal from the β -Gal/AuNP complex to restore its catalytic activity towards the fluorogenic substrate	6	Fluorescence	LDA	Proteins	1 nM	[38]
AuNPs	Competitive binding between GFP and analytes to the particle surface	8	Fluorescence	LDA	Cells, tissues	200 ng/1000 cells	[67]
AuNPs	Different aggregation behaviors and color changes when the aptamer-protected AuNPs mixed with proteins	3	Absorbance	LDA	Proteins	n.a.	[126]
AuNPs	Competitive interactions between bacterial species and the cationic AuNPs,	1	Fluorescence	LDA	Bacteria	n.a.	[149]
Col-Au NCs and Mac-Au NCs	Different interactions between proteins and the Au NCs surface	2	Fluorescence	LDA	Proteins	n.a.	[150]
AuNPs	Differential interactions between DNA-AuNPs and cells result in distinct Au growth reactions	6	Absorbance	LDA	Cells	n.a.	[129]
AuNPs	Competitive binding between DNA and proteins from the surface of AuNPs	3	Fluorescence, Absorbance	LDA, HCA	Proteins	50 nM	[127]
AuNDs	Differential interactions of proteins with AuNDs	8	Fluorescence	LDA, HCA	Proteins	n.a.	[72]
AuNPs	Competitive binding between the fluorescent proteins and the cell lysate analytes to BenzNPs	1	Fluorescence	LDA, HCA	Cells	1000 cells	[92]
AuNPs	Differential interactions of microorganisms and AuNPs caused aggregation of four sensing elements at different degrees	4	Absorbance	LDA	Microorganisms	n.a.	[28]
AuNCs	Differential interactions between free proteins and capping proteins on Au NCs	5	Phosphorescence	LDA, HCA	Proteins	n.a.	[143]
AuNPs	Different proteins triggered the DNA-protected AuNPs to exhibit different aggregation behaviors caused various solution color change	2	Absorbance	LDA, HCA	Proteins	50 nM	[128]
AuNCs	Differential binding between proteins and AuNCs resulting in the fluorescence change of AuNCs	6	Fluorescence	LDA	Proteins, serum	10 nM	[144]

Table 3. Cont.

Nanomaterials	Strategies	Numbers of ARs	Signals	Data Analysis Methods	Analytes	LOD	Ref.
AuNCs	Differential interactions between the protein and the metal ion-AuNCs	6	Fluorescence	LDA	Proteins, bacteria	n.a.	[146]
AuNPs	Aggregation of AuNPs induced by the differential metabolic capabilities of bacteria towards D-amino acids (D-AAs)	3	Absorbance	LDA, HCA	Bacteria	n.a.	[130]
AuNCs	Different oxidation of AuNCs@His by ROS	3	Fluorescence	PCA, HCA	Cells	n.a.	[147]
AuNCs	Fluorescence intensity of AuNCs was quenched to varying degrees by the bacteria	3	Fluorescence	LDA, HCA	Bacteria	10 ⁵ CFU/mL	[148]

4. Graphene Oxide (GO)-Based Sensor Arrays

GO is a chemically exfoliated graphene derivative, which can be utilized as a fluorescence quencher for various fluorescent probes, such as fluorescent polymer [76,151,152], fluorescent protein [68], metal nanodots [153], and fluorescently labeled DNA [69,154–158]. More importantly, GO showed differential affinity toward different molecules or materials [159,160]. Thus, GO has been widely applied as an ideal artificial receptor for the construction of nose/tongue sensors [71,75,150,161–166], as shown in Table 4.

Table 4. Summarization of Graphene Oxide (GO)-Based Sensor Arrays Construction Strategies with Different Artificial Receptors (ARs).

Nanomaterials	Strategies	Numbers of ARs	Signals	Data Analysis Methods	Analytes	LOD	Ref.
nGO	Proteins displace fluorophores from the nGO surface through binding competition	5	Fluorescence	LDA	Proteins	10 nM	[68]
nGO	Competitive binding between ssDNA-nGO complexes and analytes	7	Fluorescence	LDA	Proteins, cells and bacteria	5 µM	[69]
GQDs, QDs, CDs-COOH, PEI-CDs, BSA-AuNCs, Lys-AuNCs, AgNCs and GO	Competitive binding between luminescent nanodots and analytes to GO surfaces	7	Fluorescence	LDA	Proteins, bacteria	n.a.	[71]
GQDs-COOH, GQDs-NH ₂ , PEI-CDs, QDs, BSA-AuNCs, Lys-AuNCs and GO	Competitive binding between luminescent nanodots and cells to GO surfaces	6	Fluorescence	LDA	Cells	200 cells	[153]
GO	Competitive interaction among GO, AIEgen and biomolecules	7	Fluorescence	PCA	Microbes	n.a.	[167]
GO	Competitive interaction among GO, fluorescent polymers and proteins	5	Fluorescence	LDA	Proteins	n.a.	[76]
GO	Competitive binding between bacteria and GO with fluorescent PEIs	1	Fluorescence	LDA	Bacteria	OD ₆₀₀ = 0.125	[77]

The differential sensor for protein detection was developed based on GO [68]. Initially, fluorescent reporters (eGFP, pyronin Y, rhodamine 6G, acridine orange, rhodamine B) were quenched when combined to GO, and then different proteins could displace the fluorophores and restored different levels of fluorescence signal according to the affinity between GO and the proteins. In their work, a novel kind of nanoscale GO (nGOs) with a near-uniform dimension of 20 nm was applied, showing much better recognition capability than conventional GO, because nGOs have a higher supramolecular response and replacement rate. Their results showed that the nGO arrays can discriminate eight different proteins at 100 nM and 10 nM, and the success rate was as high as 95% when analyzing 48 unknowns.

Fan and co-workers combined the adaptive “ensemble aptamers” (ENSaptamers) and nGOs to develop a sensor array for high-precision identification of proteins, bacteria, and cells [69]. Auguste and co-workers provided a sensing array for the identification of healthy, cancerous, and metastatic human breast cells using six luminescent nanodot-graphene oxide complexes as novel fluorescent nanoprobe [153]. The sensing system was disrupted in the presence of breast cells, producing a distinct fluorescence response pattern. The multichannel sensor was capable of effectively identifying healthy, cancerous, and metastatic human breast cells with as few as 200 cells. Tomita and co-workers constructed a cross-reactive DNA-based array for one-step identification of antibody degradation pathways. The signature-based sensing platform was able to identify a broad range of degraded antibodies, such as common features of native, denatured, and visibly aggregated antibodies, complicated degradation pathways of therapeutic omalizumab upon time-course heat-treatment, and the individual compositions of differently degraded omalizumab mixtures. Tang and Qin [167] developed a microbial lysate-responsive fluorescent sensor array using luminogens featuring aggregation-induced emission characteristics (AIEgens) and graphene oxide (GO). This combination effectively reduces background signals and enhances discrimination ability through competitive interactions among AIEgens, microbial lysates, and GO. The sensor array successfully identified six microbes, including fungi, Gram-positive bacteria, and Gram-negative bacteria.

Han and co-workers [77] developed a novel multichannel array using modified polyethyleneimine and graphene oxide. This complex system enabled the successful identification of 10 bacteria within minutes through electrostatic and hydrophobic interactions. The sensor array also demonstrated the ability to measure bacterial concentrations and identify mixed bacteria accurately. In biological samples such as urine, the array achieved high accuracy. Han and co-workers [76] also designed five positively charged poly(para-aryleneethynylene) (P1–P5) molecules to form electrostatic complexes (C1–C5) with negatively charged graphene oxide (GO), effectively distinguishing between 12 proteins while employing machine learning algorithms. Moreover, these sensor arrays accurately identified levels of A β 40 and A β 42 aggregates, including monomers, oligomers, and fibrils, offering an attractive strategy for early Alzheimer’s disease diagnosis (Figure 4).

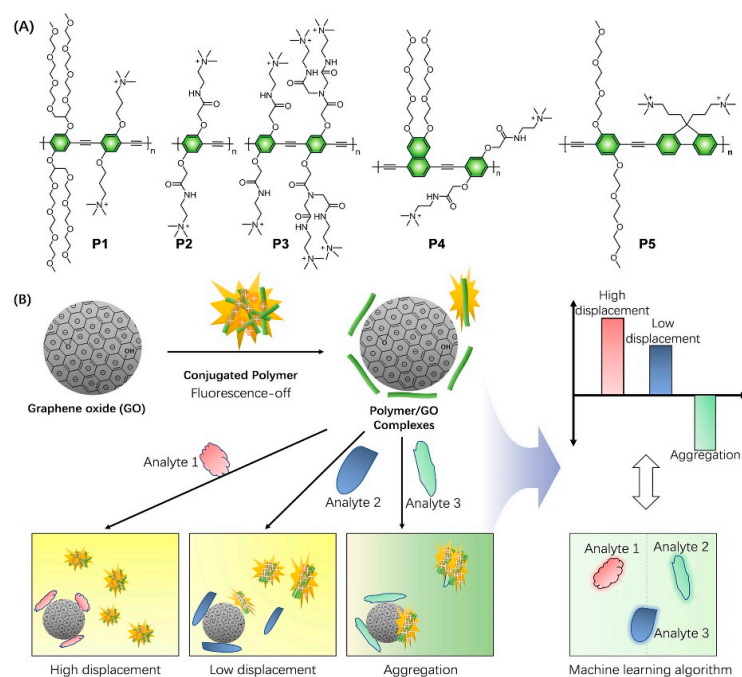


Figure 4. (A) Chemical structures of fluorescent polymers P1–P5. (B) Schematic illustration of the construction of electrostatic complexes from positively charged poly(para-aryleneethynylene)s and negatively charged GO and identification mechanism for multiple analytes. Reprinted with permission from [76]. Copyright 2022 American Chemical Society.

5. Quantum Dot (QD)-Based Sensor Arrays

Based on their distinguished characteristics of good photostability, high quantum yield, and long fluorescence lifetime, QDs have been extensively used in fluorescent bioanalysis [161,168–171]. Rotello and co-workers developed a QD-based sensor for sensing mammalian cell types and states [100]. The sensing system is composed of two quantum dots and one gold nanoparticle. The quantum dots serve as transducers, which can be quenched by the gold nanoparticle. Different cell types and states were successfully differentiated by the sensor array (Figure 5).

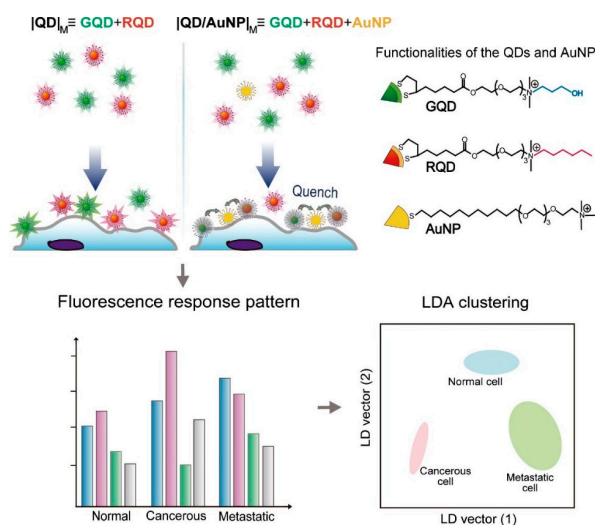


Figure 5. Illustration showing how nanoparticles interact with the cell surface in a sensing system, resulting in differential quenching and distinct patterns for distinguishing different cell types/states. Reprinted with permission from [100]. 2012 Elsevier Ireland Ltd. All rights reserved.

Wang and Chen developed a fluorescent sensor array using imidazolium ionic liquids (ILs) and ionic liquid-QD conjugates as semi-selective receptors for the discrimination of proteins [172]. The IL sensing system was able to differentiate eight proteins at a concentration of 500 nM with an accuracy of 91.7%. With the improvements of the sensitivity and discrimination accuracy, the IL@QDs/QDs sensing system could distinguish eight proteins with 100% accuracy at a very low concentration of 10 nM. Additionally, protein mixtures and proteins spiked in human urine were well-discriminated by the IL@QDs/QDs sensing system.

Yan and co-workers designed a multidimensional sensing device based on Mn-ZnS QDs for the discrimination of proteins [173]. The triple-channel optical properties (fluorescence, phosphorescence, light scattering) of Mn-ZnS QDs were utilized to achieve the output signals. After interaction with target proteins, the changes in the triple-channel optical properties of Mn-ZnS QDs were observed. The multidimensional sensing devices were able to generate distinct patterns for different proteins. Eight proteins added to human urine samples were successfully discriminated against with the aid of principal component analysis.

Combination of different nanomaterials, Wu and Zhang developed a nanoparticle quantum dot-based fluorescence sensor array for sensing proteins and cancer cells [174]. The sensor array consists of six types of nanoparticles (NPs, including CuO, ZnO, Eu₂O₃, AuNPs, AgNPs, Au-Ag core-shell) and CdSe quantum dots (Figure 6). These NPs can quench the fluorescence of CdSe quantum dots. The NP-QD interaction was disrupted by the addition of proteins, leading to fluorescence turn-on or further quenching. Eight proteins were readily differentiated by using LDA analysis. Moreover, protein quantification was achieved with the limits of detection below 2 μ M in the range of 2–50 μ M. Qu and Ren [71] designed seven fluorescent luminescent nanoprobe, including graphene quantum dots (GQDs), CdTe quantum dots (QDs), carboxyl-carbon dots (CDs-COOH), polyethyleneimine functionalized carbon dots (PEI-CDs), BSA-templated gold nanoclusters (BSA-AuNCs), lysozyme-templated gold nanoclusters (LysAuNCs), and DNA-templated silver nanoclusters (AgNCs), and they used graphene oxide (GO) as an excellent quencher with different affinity to proteins and the nanoprobe. The discrimination ability of this array was tested by analyzing eight proteins at low concentrations. Finally, 100% accuracy was achieved for the identification of 48 unknown protein samples. The summary of quantum dot (QD)-based sensor arrays is shown in Table 5.

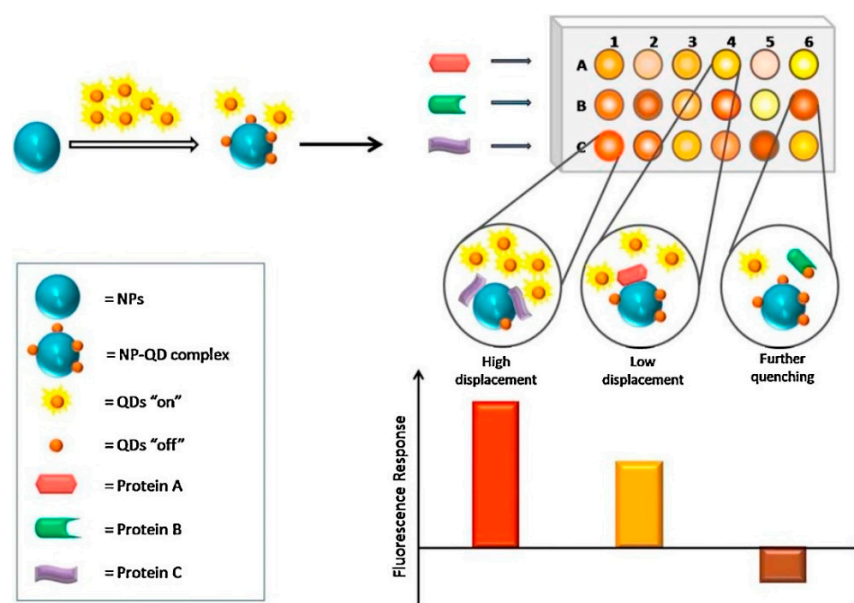


Figure 6. Schematic illustration of a fluorescence sensor array based on six types of NP-QD complexes. Reprinted with permission from [174]; 2017 Elsevier B.V. All rights reserved.

Table 5. Summarization of Quantum dot (QD)-based Sensor Arrays Construction Strategies with Different Artificial Receptors (ARs).

Nanomaterials	Strategies	Numbers of ARs	Signals	Data Analysis Methods	Analytes	LOD	Ref.
Mn–ZnS QDs	Different interactions of Mn–ZnS QDs with proteins	1	Fluorescence phosphorescence light scattering	PCA	Proteins	0.5 μ M	[173]
QDs	Differential competitive and selective non-covalent interactions between nanoparticles and cell surface	2	Fluorescence	LDA	Cells	10,000 cells	[100]
CdTe QDs	Differential interactions between analytes and IL@CdTe QDs	5	Fluorescence	LDA	Proteins, bacteria	10 nM	[175]
CuO NPs, ZnO NPs, Eu ₂ O ₃ NPs, AuNPs, AgNPs, Au–Ag core-shell and CdSe QDs	Protein presence disrupts nanoparticle-QD interactions, resulting in fluorescence turn on or further quenching	6	Fluorescence	LDA	Proteins, cells	5 μ M	[174]

6. Other Metal Nanoparticle-Based Sensor Arrays

Other metal nanoparticles, such as Fe₃O₄ NPs, AgNPs, MoS₂, and CuS NPs, were also prepared to develop sensor arrays for the discrimination of proteins, bacteria, and cells [78,176–183]. Scientists fabricated dopamine and trimethylammonium functionalized Fe₃O₄ NPs, which were able to catalyze the oxidation of colorless ABTS to become a green product in the presence of H₂O₂ [66]. When analyte proteins were added into the mixture, the accessibility of reaction substrates to the NP surface was adjusted, leading to a change in the catalytic efficiency. The Fe₃O₄ NP-based sensor array can identify ten proteins at a concentration of 50 nM. Cui and co-workers developed a dynamically tunable, low-background, and highly reproducible CL system based on luminol-functionalized silver nanoparticles (luminol-AgNPs) for protein sensing [184]. Qu and Ren also utilized AgNPs to construct sensor arrays for the recognition of proteins [185]. Although AgNPs have some unique properties, their instability and toxicity limit their application in bioanalysis. Ren and Pu developed a sensor array for the identification of proteins and antibiotic-resistant bacteria utilizing CuS NPs and fluorescent dyes [186]. The sensing platform showed excellent discrimination ability between antibiotic-resistant and antibiotic-susceptible bacteria extracts.

Zhang and coworkers constructed quaternized magnetic nanoparticle (q-MNP)-fluorescent polymer systems for the detection and identification of bacteria [187]. The complexes of the q-MNP-fluorescent polymer were disrupted by the bacterial cell membranes, leading to a unique fluorescence response. Eight bacteria were quantitatively discriminated with LDA with an accuracy of 87.5% for 10⁷ cfu/mL within 20 min. The sensor array was also used to identify 32 unknown bacteria samples with an accuracy of 96.8%. The summarization of the other metal nanoparticle-based sensor arrays is shown in Table 6.

Table 6. Summarization of the Sensor Arrays Construction Strategies with Different Artificial Receptors (ARs).

Nanomaterials	Strategies	Numbers of ARs	Signals	Data Analysis Methods	Analytes	LOD	Ref.
Fe ₃ O ₄ NPs	Differential interactions of proteins with Fe ₃ O ₄ NPs affected the accessibility of ABTS to the NP surface	2	Fluorescence	LDA	Proteins	50 nM	[66]

Table 6. Cont.

Nanomaterials	Strategies	Numbers of ARs	Signals	Data Analysis Methods	Analytes	LOD	Ref.
AgNPs	Different adsorption capacity of proteins onto luminol-AgNPs affected the accessibility of H ₂ O ₂ to the NPs surface	1	Chemiluminescence	PCA	Proteins	n.a.	[184]
Quaternized magnetic nanoparticles (q-MNP)	Competitive binding between fluorescent polymer and bacteria to GO surfaces q-MNP	3	Fluorescence	LDA	Bacteria	n.a.	[187]
CuS NPs	Competitive binding between analytes and fluorescent dyes towards CuS NPs	4	Fluorescence	PCA	Proteins, bacteria	n.a.	[186]
AgNPs	The diversity in structure and properties of various proteins results in different effects on the synthesis of AgNPs under light irradiation, leading to AgNPs with distinct LSPR absorption spectra	3	Absorbance	PCA	Proteins	n.a.	[185]
DBCO-UCNPs	Different bacteria exhibit differences in metabolic capability, sensitivity to antibiotics, and surface properties and thus lead to discriminative responses	6	Fluorescence	PCA, HCA, LDA	Bacteria	10 ⁵ CFU/mL	[34]

7. Conclusions

The integration of nanomaterials in optical differential sensors has provided a powerful platform for biosystems analysis [188]. In contrast to traditional lock-and-key biosensing, these sensors function as chemical noses with the ability to recognize a wide range of targets, including proteins, mammalian cells, and microorganisms [189].

The use of nanomaterials has expanded the design possibilities of analysis arrays in several significant ways. Firstly, more different molecular assembly modes and larger assembly quantities are now achievable using covalent bonding modifications or surface adsorption, etc. Secondly, nanomaterials themselves possess more diverse signal outputs, such as the abundant fluorescence signals of quantum dots at various wavelengths or the color changes of nanogold particles. Thirdly, nanomaterials provide a wider range of interaction mechanisms between nanointerfaces and biomolecules, reflecting surface charge and molecular structure, etc. Lastly, the application of hierarchical nanomaterials further enhances the capabilities of analysis arrays. By combining hierarchical nanomaterials, additional advantages for biosensing applications can be achieved. These materials improve signal intensity and enhance various energy transfer processes. The integration of hierarchical nanomaterials alongside other nanomaterials expands the design possibilities of analysis arrays, enabling even more diverse and efficient biosensing platforms [190]. Overall, the application of nanomaterials has dramatically improved the sensitivity and recognition range of pattern recognition detection, leading to more diverse array designs [191]. However, challenges remain in this field.

Future research directions and urgent issues include: (1) Further theoretical studies are needed to understand the signal mechanisms of most sensing arrays. (2) To radically improve the accuracy of pattern recognition, the stability and controllability of the nanomaterials are critical. (3) Further enhance the discrimination ability and sensitivity of pattern recognition sensors. (4) Efforts should be made to reduce the production cost of nanoprobables to decrease expenses associated with their use. (5) The application of interfacial

self-assembly on micro/nanochip technology should be helpful for the high-throughput data collection for next-generation chemical noses. (6) The introduction of novel and superior nanomaterials would greatly improve the performance of the sensor array. For example, single-chirality carbon nanotubes are recently drawing a large amount of research interest for their near-infrared fluorescence signals and specific recognition and binding abilities for biomolecules. Addressing these challenges and capitalizing on emerging advancements will undoubtedly contribute to the continuous progress of this field.

Author Contributions: Conceptualization, L.W., L.L., X.Y. and Q.T.; resources and data curation, L.L., X.Y., M.C. and Q.T.; writing—original draft preparation, L.W., Q.T., X.S. and M.C.; writing—review and editing, L.W., Y.W., W.L. and G.L.; visualization, L.W. and X.S.; supervision, Y.W. and G.L.; project administration, W.L. and X.S.; funding acquisition, Y.W. and G.L. All authors have read and agreed to the published version of the manuscript.

Funding: This work was financially supported by the National Quality Infrastructure Program of China (2021YFF0600901 NQI) and the National Natural Science Foundation of China (No. 22074093).

Institutional Review Board Statement: Not applicable.

Informed Consent Statement: Not applicable.

Data Availability Statement: Not applicable.

Conflicts of Interest: The authors declare no conflict of interest.

References

1. Rodriguez, R.S.; O’Keefe, T.L.; Froehlich, C.; Lewis, R.E.; Sheldon, T.R.; Haynes, C.L. Sensing Food Contaminants: Advances in Analytical Methods and Techniques. *Anal. Chem.* **2021**, *93*, 23–40. [[CrossRef](#)]
2. Shruti, A.; Bage, N.; Kar, P. Nanomaterials based sensors for analysis of food safety. *Food Chem.* **2024**, *433*, 137284. [[CrossRef](#)]
3. Pan, M.F.; Yin, Z.J.; Liu, K.X.; Du, X.L.; Liu, H.L.; Wang, S. Carbon-Based Nanomaterials in Sensors for Food Safety. *Nanomaterials* **2019**, *9*, 1330. [[CrossRef](#)]
4. Lv, M.; Liu, Y.; Geng, J.H.; Kou, X.H.; Xin, Z.H.; Yang, D.Y. Engineering nanomaterials-based biosensors for food safety detection. *Biosens. Bioelectron.* **2018**, *106*, 122–128. [[CrossRef](#)]
5. Huang, Y.K.; Mei, L.; Chen, X.G.; Wang, Q. Recent Developments in Food Packaging Based on Nanomaterials. *Nanomaterials* **2018**, *8*, 830. [[CrossRef](#)]
6. Chu, H.Q.; Lu, Y.F. Application of Functional Nanomaterials in Food Safety. *Chin. J. Anal. Chem.* **2010**, *38*, 442–448. [[CrossRef](#)]
7. Wen, Y.; Wang, L.; Xu, L.; Li, L.; Ren, S.; Cao, C.; Jia, N.; Aldalbahi, A.; Song, S.; Shi, J.; et al. Electrochemical detection of PCR amplicons of Escherichia coli genome based on DNA nanostructural probes and polyHRP enzyme. *Analyst* **2016**, *141*, 5304–5310. [[CrossRef](#)]
8. Yang, X.; Wen, Y.; Wang, L.; Zhou, C.; Li, Q.; Xu, L.; Li, L.; Shi, J.; Lal, R.; Ren, S.; et al. PCR-Free Colorimetric DNA Hybridization Detection Using a 3D DNA Nanostructured Reporter Probe. *ACS Appl. Mater. Interfaces* **2017**, *9*, 38281–38287. [[CrossRef](#)]
9. Li, L.; Wang, L.; Xu, Q.; Xu, L.; Liang, W.; Li, Y.; Ding, M.; Aldalbahi, A.; Ge, Z.; Wang, L.; et al. Bacterial Analysis Using an Electrochemical DNA Biosensor with Poly-Adenine-Mediated DNA Self-Assembly. *ACS Appl. Mater. Interfaces* **2018**, *10*, 6895–6903. [[CrossRef](#)]
10. Bayramoglu, G.; Ozalp, V.C.; Dincbal, U.; Arica, M.Y. Fast and Sensitive Detection of Salmonella in Milk Samples Using Aptamer-Functionalized Magnetic Silica Solid Phase and MCM-41-Aptamer Gate System. *ACS Biomater. Sci. Eng.* **2018**, *4*, 1437–1444. [[CrossRef](#)]
11. Wang, L.; Wen, Y.; Yang, X.; Xu, L.; Liang, W.; Zhu, Y.; Wang, L.; Li, Y.; Li, Y.; Ding, M.; et al. Ultrasensitive Electrochemical DNA Biosensor Based on a Label-Free Assembling Strategy Using a Triblock polyA DNA Probe. *Anal. Chem.* **2019**, *91*, 16002–16009. [[CrossRef](#)] [[PubMed](#)]
12. da Costa, B.M.C.; Duarte, A.C.; Rocha-Santos, T.A.P. Environmental monitoring approaches for the detection of organic contaminants in marine environments: A critical review. *Trends Environ. Anal. Chem.* **2022**, *33*, e00154. [[CrossRef](#)]
13. Liang, M.M.; Guo, L.H. Application of Nanomaterials in Environmental Analysis and Monitoring. *J. Nanosci. Nanotechnol.* **2009**, *9*, 2283–2289. [[CrossRef](#)] [[PubMed](#)]
14. Farzin, L.; Shamsipur, M.; Sheibani, S. A review: Aptamer-based analytical strategies using the nanomaterials for environmental and human monitoring of toxic heavy metals. *Talanta* **2017**, *174*, 619–627. [[CrossRef](#)] [[PubMed](#)]
15. Abu, H.; Hossain, M.A.M.; Marlinda, A.; Al Mamun, M.; Simarani, K.; Johan, M.R. Nanomaterials based electrochemical nucleic acid biosensors for environmental monitoring: A review. *Appl. Surf. Sci. Adv.* **2021**, *4*, 100064. [[CrossRef](#)]
16. Wang, L.; Wen, Y.; Li, L.; Yang, X.; Jia, N.; Li, W.; Meng, J.; Duan, M.; Sun, X.; Liu, G. Sensitive and label-free electrochemical lead ion biosensor based on a DNAzyme triggered G-quadruplex/hemin conformation. *Biosens. Bioelectron.* **2018**, *115*, 91–96. [[CrossRef](#)] [[PubMed](#)]

17. Lotfi Zadeh Zhad, H.R.; Lai, R.Y. Application of Calcium-Binding Motif of E-Cadherin for Electrochemical Detection of Pb(II). *Anal. Chem.* **2018**, *90*, 6519–6525. [[CrossRef](#)]
18. Wang, L.Q.; Wang, X.J.; Wu, Y.G.; Guo, M.Q.; Gu, C.J.; Dai, C.H.; Kong, D.R.; Wang, Y.; Zhang, C.; Qu, D.; et al. Rapid and ultrasensitive electromechanical detection of ions, biomolecules and SARS-CoV-2 RNA in unamplified samples. *Nat. Biomed. Eng.* **2022**, *6*, 276–285. [[CrossRef](#)]
19. Song, P.; Shen, J.W.; Ye, D.K.; Dong, B.J.; Wang, F.; Pei, H.; Wang, J.B.; Shi, J.Y.; Wang, L.H.; Xue, W.; et al. Programming bulk enzyme heterojunctions for biosensor development with tetrahedral DNA framework. *Nat. Commun.* **2022**, *13*, 1917. [[CrossRef](#)]
20. Zhai, T.T.; Wei, Y.H.; Wang, L.H.; Li, J.; Fan, C.H. Advancing pathogen detection for airborne diseases. *Fundam. Res.* **2023**, *3*, 520–524. [[CrossRef](#)]
21. Wang, L.; Dong, L.; Liu, G.; Shen, X.; Wang, J.; Zhu, C.; Ding, M.; Wen, Y. Fluorometric determination of HIV DNA using molybdenum disulfide nanosheets and exonuclease III-assisted amplification. *Mikrochim. Acta* **2019**, *186*, 286. [[CrossRef](#)]
22. Zhang, Y.; Shuai, Z.; Zhou, H.; Luo, Z.; Liu, B.; Zhang, Y.; Zhang, L.; Chen, S.; Chao, J.; Weng, L.; et al. Single-Molecule Analysis of MicroRNA and Logic Operations Using a Smart Plasmonic Nanobiosensor. *J. Am. Chem. Soc.* **2018**, *140*, 3988–3993. [[CrossRef](#)]
23. Yang, F.; Li, Q.; Wang, L.; Zhang, G.J.; Fan, C. Framework-Nucleic-Acid-Enabled Biosensor Development. *ACS Sens.* **2018**, *3*, 903–919. [[CrossRef](#)]
24. Zhao, R.; Lv, M.; Li, Y.; Sun, M.; Kong, W.; Wang, L.; Song, S.; Fan, C.; Jia, L.; Qiu, S.; et al. Stable Nanocomposite Based on PEGylated and Silver Nanoparticles Loaded Graphene Oxide for Long-Term Antibacterial Activity. *ACS Appl. Mater. Interfaces* **2017**, *9*, 15328–15341. [[CrossRef](#)]
25. Yin, F.; Zhao, H.; Lu, S.; Shen, J.; Li, M.; Mao, X.; Li, F.; Shi, J.; Li, J.; Dong, B.; et al. DNA-framework-based multidimensional molecular classifiers for cancer diagnosis. *Nat. Nanotechnol.* **2023**, *18*, 677–686. [[CrossRef](#)]
26. Mao, D.; Dong, Z.; Liu, X.; Li, W.; Li, H.; Gu, C.; Chen, G.; Zhu, X.; Yang, Y. Intelligent DNA nanoreactor for in vivo easy-to-read tumor imaging and precise therapy. *Angew. Chem. Int. Ed. Engl.* **2023**, *63*, e202311309. [[CrossRef](#)]
27. Li, Y.; Wen, Y.; Wang, L.; Liang, W.; Xu, L.; Ren, S.; Zou, Z.; Zuo, X.; Fan, C.; Huang, Q.; et al. Analysis of telomerase activity based on a spired DNA tetrahedron TS primer. *Biosens. Bioelectron.* **2015**, *67*, 364–369. [[CrossRef](#)]
28. Qian, Y.; Fan, T.; Wang, P.; Zhang, X.; Luo, J.; Zhou, F.; Yao, Y.; Liao, X.; Li, Y.; Gao, F. A novel label-free homogeneous electrochemical immunosensor based on proximity hybridization-triggered isothermal exponential amplification induced G-quadruplex formation. *Sens. Actuators B Chem.* **2017**, *248*, 187–194. [[CrossRef](#)]
29. Zhang, L.; Wang, J.; Zhang, J.; Liu, Y.; Wu, L.; Shen, J.; Zhang, Y.; Hu, Y.; Fan, Q.; Huang, W.; et al. Individual Au-Nanocube Based Plasmonic Nanoprobe for Cancer Relevant MicroRNA Biomarker Detection. *ACS Sens.* **2017**, *2*, 1435–1440. [[CrossRef](#)] [[PubMed](#)]
30. Zhang, L.; Zhang, Y.; Hu, Y.; Fan, Q.; Yang, W.; Li, A.; Li, S.; Huang, W.; Wang, L. Refractive index dependent real-time plasmonic nanoprobe on a single silver nanocube for ultrasensitive detection of the lung cancer-associated miRNAs. *Chem. Commun.* **2015**, *51*, 294–297. [[CrossRef](#)] [[PubMed](#)]
31. Zhou, X.; Zhao, M.; Duan, X.; Guo, B.; Cheng, W.; Ding, S.; Ju, H. Collapse of DNA Tetrahedron Nanostructure for “Off-On” Fluorescence Detection of DNA Methyltransferase Activity. *ACS Appl. Mater. Interfaces* **2017**, *9*, 40087–40093. [[CrossRef](#)] [[PubMed](#)]
32. Beard, D.J.; Perrine, S.A.; Phillips, E.; Hoque, S.; Conerly, S.; Tichenor, C.; Simmons, M.A.; Young, J.K. Conformational comparisons of a series of tachykinin peptide analogs. *J. Med. Chem.* **2007**, *50*, 6501–6506. [[CrossRef](#)] [[PubMed](#)]
33. Li, T.; Zhu, X.; Hai, X.; Bi, S.; Zhang, X. Recent Progress in Sensor Arrays: From Construction Principles of Sensing Elements to Applications. *ACS Sens.* **2023**, *8*, 994–1016. [[CrossRef](#)] [[PubMed](#)]
34. Wang, X.; Li, H.; Yang, J.; Wu, C.; Chen, M.; Wang, J.; Yang, T. Chemical Nose Strategy with Metabolic Labeling and “Antibiotic-Responsive Spectrum” Enables Accurate and Rapid Pathogen Identification. *Anal. Chem.* **2024**, *96*, 427–436. [[CrossRef](#)] [[PubMed](#)]
35. Liu, J.B.; Li, G.; Yang, X.H.; Wang, K.M.; Li, L.; Liu, W.; Shi, X.; Guo, Y.L. Exciton Energy Transfer-Based Quantum Dot Fluorescence Sensing Array: “Chemical Noses” for Discrimination of Different Nucleobases. *Anal. Chem.* **2015**, *87*, 876–883. [[CrossRef](#)] [[PubMed](#)]
36. Li, L.; Li, G.; He, X.X.; Yang, X.H.; Liu, S.Y.; Tang, J.L.; Chen, Q.S.; Liu, J.B.; Wang, K.M. Protein-driven disassembly of surfactant-polyelectrolyte nanomicelles: Modulation of quantum dot/fluorochrome FRET for pattern sensing. *Sens. Actuators B-Chem.* **2018**, *272*, 393–399. [[CrossRef](#)]
37. Li, Z.; Askim, J.R.; Suslick, K.S. The Optoelectronic Nose: Colorimetric and Fluorometric Sensor Arrays. *Chem. Rev.* **2019**, *119*, 231–292. [[CrossRef](#)]
38. Miranda, O.R.; Chen, H.-T.; You, C.-C.; Mortenson, D.E.; Yang, X.-C.; Bunz, U.H.F.; Rotello, V.M. Enzyme-Amplified Array Sensing of Proteins in Solution and in Biofluids. *J. Am. Chem. Soc.* **2010**, *132*, 5285–5289. [[CrossRef](#)]
39. Yan, Q.; Ding, X.Y.; Chen, Z.H.; Xue, S.F.; Han, X.Y.; Lin, Z.Y.; Yang, M.; Shi, G.; Zhang, M. pH-Regulated Optical Performances in Organic/Inorganic Hybrid: A Dual-Mode Sensor Array for Pattern-Recognition-Based Biosensing. *Anal. Chem.* **2018**, *90*, 10536–10542. [[CrossRef](#)]
40. Mei, Y.; Zhang, Q.W.; Gu, Q.; Liu, Z.; He, X.; Tian, Y. Pillar[5]arene-Based Fluorescent Sensor Array for Biosensing of Intracellular Multi-neurotransmitters through Host-Guest Recognitions. *J. Am. Chem. Soc.* **2022**, *144*, 2351–2359. [[CrossRef](#)]
41. Yao, J.; Yang, M.; Duan, Y.X. Chemistry, Biology, and Medicine of Fluorescent Nanomaterials and Related Systems: New Insights into Biosensing, Bioimaging, Genomics, Diagnostics, and Therapy. *Chem. Rev.* **2014**, *114*, 6130–6178. [[CrossRef](#)]
42. Meng, H.M.; Liu, H.; Kuai, H.L.; Peng, R.Z.; Mo, L.T.; Zhang, X.B. Aptamer-integrated DNA nanostructures for biosensing, bioimaging and cancer therapy. *Chem. Soc. Rev.* **2016**, *45*, 2583–2602. [[CrossRef](#)]

43. Zhang, S.D.; Geryak, R.; Geldmeier, J.; Kim, S.; Tsukruk, V.V. Synthesis, Assembly, and Applications of Hybrid Nanostructures for Biosensing. *Chem. Rev.* **2017**, *117*, 12942–13038. [[CrossRef](#)]
44. Sun, H.J.; Zhou, Y.; Ren, J.S.; Qu, X.G. Carbon Nanozymes: Enzymatic Properties, Catalytic Mechanism, and Applications. *Angew. Chem.-Int. Ed.* **2018**, *57*, 9224–9237. [[CrossRef](#)]
45. Yadav, V.; Roy, S.; Singh, P.; Khan, Z.; Jaiswal, A. 2D MoS₂-Based Nanomaterials for Therapeutic, Bioimaging, and Biosensing Applications. *Small* **2019**, *15*, e1803706. [[CrossRef](#)]
46. Ji, C.Y.; Zhou, Y.Q.; Leblanc, R.M.; Peng, Z.L. Recent Developments of Carbon Dots in Biosensing: A Review. *ACS Sens.* **2020**, *5*, 2724–2741. [[CrossRef](#)]
47. Chung, S.; Revia, R.A.; Zhang, M.Q. Graphene Quantum Dots and Their Applications in Bioimaging, Biosensing, and Therapy. *Adv. Mater.* **2021**, *33*, e1904362. [[CrossRef](#)]
48. Xu, W.Q.; Jiao, L.; Wu, Y.; Hu, L.Y.; Gu, W.L.; Zhu, C.Z. Metal-Organic Frameworks Enhance Biomimetic Cascade Catalysis for Biosensing. *Adv. Mater.* **2021**, *33*, 2005172. [[CrossRef](#)]
49. Kumar, S.; Wang, Z.; Zhang, W.; Liu, X.C.; Li, M.Y.; Li, G.R.; Zhang, B.Y.; Singh, R. Optically Active Nanomaterials and Its Biosensing Applications-A Review. *Biosensors* **2023**, *13*, 85. [[CrossRef](#)]
50. Pini, F.; Francés-Soriano, L.; Andriago, V.; Natile, M.M.; Hildebrandt, N. Optimizing Upconversion Nanoparticles for FRET Biosensing. *ACS Nano* **2023**, *17*, 4971–4984. [[CrossRef](#)]
51. Du, H.; Xie, Y.Q.; Wang, J. Nanomaterial-sensors for herbicides detection using electrochemical techniques and prospect applications. *Trac-Trends Anal. Chem.* **2021**, *135*, 116178. [[CrossRef](#)]
52. Zhai, T.T.; Zheng, H.R.; Fang, W.N.; Gao, Z.S.; Song, S.P.; Zuo, X.L.; Li, Q.; Wang, L.H.; Li, J.; Shi, J.Y.; et al. DNA-Encoded Gold-Gold Wettability for Programmable Plasmonic Engineering. *Angew. Chem.-Int. Ed.* **2022**, *61*, e202210377. [[CrossRef](#)]
53. Unser, S.; Bruzas, I.; He, J.; Sagle, L. Localized Surface Plasmon Resonance Biosensing: Current Challenges and Approaches. *Sensors* **2015**, *15*, 15684–15716. [[CrossRef](#)]
54. Wang, H.S. Metal-organic frameworks for biosensing and bioimaging applications. *Coord. Chem. Rev.* **2017**, *349*, 139–155. [[CrossRef](#)]
55. Loiseau, A.; Asila, V.; Boitel-Aullen, G.; Lam, M.; Salmain, M.; Boujday, S. Silver-Based Plasmonic Nanoparticles for and Their Use in Biosensing. *Biosensors* **2019**, *9*, 78. [[CrossRef](#)]
56. Xu, W.Q.; Jiao, L.; Yan, H.Y.; Wu, Y.; Chen, L.J.; Gu, W.L.; Du, D.; Lin, Y.H.; Zhu, C.Z. Glucose Oxidase-Integrated Metal-Organic Framework Hybrids as Biomimetic Cascade Nanozymes for Ultrasensitive Glucose Biosensing. *ACS Appl. Mater. Interfaces* **2019**, *11*, 22096–22101. [[CrossRef](#)]
57. De los Santos, Z.A.; Lin, Z.W.; Zheng, M. Optical Detection of Stereoselective Interactions with DNA-Wrapped Single-Wall Carbon Nanotubes. *J. Am. Chem. Soc.* **2021**, *143*, 20628–20632. [[CrossRef](#)]
58. Lim, S.Y.; Shen, W.; Gao, Z.Q. Carbon quantum dots and their applications. *Chem. Soc. Rev.* **2015**, *44*, 362–381. [[CrossRef](#)]
59. Ahn, N.; Livache, C.; Pinchetti, V.; Jung, H.; Jin, H.; Hahm, D.; Park, Y.S.; Klimov, V.I. Electrically driven amplified spontaneous emission from colloidal quantum dots. *Nature* **2023**, *617*, 79–85. [[CrossRef](#)]
60. Wu, P.; Yan, X.P. Doped quantum dots for chemo/biosensing and bioimaging. *Chem. Soc. Rev.* **2013**, *42*, 5489–5521. [[CrossRef](#)]
61. Wu, P.; Hou, X.D.; Xu, J.J.; Chen, H.Y. Ratiometric fluorescence, electrochemiluminescence, and photoelectrochemical chemo/biosensing based on semiconductor quantum dots. *Nanoscale* **2016**, *8*, 8427–8442. [[CrossRef](#)]
62. Sun, J.W.; Lu, Y.X.; He, L.Y.; Pang, J.W.; Yang, F.Y.; Liu, Y.Y. Colorimetric sensor array based on gold nanoparticles: Design principles and recent advances. *Trac-Trends Anal. Chem.* **2020**, *122*, 115754. [[CrossRef](#)]
63. Behera, P.; De, M. Nanomaterials in Optical Array-Based Sensing. In *Organic and Inorganic Materials Based Sensors*; Wiley: New York, NY, USA, 2024; pp. 495–533. [[CrossRef](#)]
64. Naresh, V.; Lee, N. A Review on Biosensors and Recent Development of Nanostructured Materials-Enabled Biosensors. *Sensors* **2021**, *21*, 1109. [[CrossRef](#)]
65. You, C.C.; Miranda, O.R.; Gider, B.; Ghosh, P.S.; Kim, I.B.; Erdogan, B.; Krovi, S.A.; Bunz, U.H.; Rotello, V.M. Detection and identification of proteins using nanoparticle-fluorescent polymer ‘chemical nose’ sensors. *Nat. Nanotechnol.* **2007**, *2*, 318–323. [[CrossRef](#)]
66. Li, X.N.; Wen, F.; Creran, B.; Jeong, Y.D.; Zhang, X.R.; Rotello, V.M. Colorimetric Protein Sensing Using Catalytically Amplified Sensor Arrays. *Small* **2012**, *8*, 3589–3592. [[CrossRef](#)]
67. Rana, S.; Singla, A.K.; Bajaj, A.; Elci, S.G.; Miranda, O.R.; Mout, R.; Yan, B.; Jirik, F.R.; Rotello, V.M. Array-Based Sensing of Metastatic Cells and Tissues Using Nanoparticle-Fluorescent Protein Conjugates. *ACS Nano* **2012**, *6*, 8233–8240. [[CrossRef](#)]
68. Chou, S.S.; De, M.; Luo, J.Y.; Rotello, V.M.; Huang, J.X.; Dravid, V.P. Nanoscale Graphene Oxide (nGO) as Artificial Receptors: Implications for Biomolecular Interactions and Sensing. *J. Am. Chem. Soc.* **2012**, *134*, 16725–16733. [[CrossRef](#)]
69. Pei, H.; Li, J.; Lv, M.; Wang, J.; Gao, J.; Lu, J.; Li, Y.; Huang, Q.; Hu, J.; Fan, C. A graphene-based sensor array for high-precision and adaptive target identification with ensemble aptamers. *J. Am. Chem. Soc.* **2012**, *134*, 13843–13849. [[CrossRef](#)]
70. Xu, S.; Lu, X.; Yao, C.; Huang, F.; Jiang, H.; Hua, W.; Na, N.; Liu, H.; Ouyang, J. A Visual Sensor Array for Pattern Recognition Analysis of Proteins Using Novel Blue-Emitting Fluorescent Gold Nanoclusters. *Anal. Chem.* **2014**, *86*, 11634–11639. [[CrossRef](#)]
71. Tao, Y.; Ran, X.; Ren, J.S.; Qu, X.G. Array-Based Sensing of Proteins and Bacteria By Using Multiple Luminescent Nanodots as Fluorescent Probes. *Small* **2014**, *10*, 3667–3671. [[CrossRef](#)]

72. Yuan, Z.; Du, Y.; Tseng, Y.T.; Peng, M.; Cai, N.; He, Y.; Chang, H.T.; Yeung, E.S. Fluorescent gold nanodots based sensor array for proteins discrimination. *Anal. Chem.* **2015**, *87*, 4253–4259. [[CrossRef](#)]
73. Xu, Q.; Zhang, Y.; Tang, B.; Zhang, C.-y. Multicolor Quantum Dot-Based Chemical Nose for Rapid and Array-Free Differentiation of Multiple Proteins. *Anal. Chem.* **2016**, *88*, 2051–2058. [[CrossRef](#)]
74. Li, B.Y.; Li, X.Z.; Dong, Y.H.; Wang, B.; Li, D.Y.; Shi, Y.M.; Wu, Y.Y. Colorimetric Sensor Array Based on Gold Nanoparticles with Diverse Surface Charges for Microorganisms Identification. *Anal. Chem.* **2017**, *89*, 10639–10643. [[CrossRef](#)]
75. Qiu, H.; Pu, F.; Ran, X.; Liu, C.; Ren, J.; Qu, X. Nanozyme as Artificial Receptor with Multiple Readouts for Pattern Recognition. *Anal. Chem.* **2018**, *90*, 11775–11779. [[CrossRef](#)]
76. Wang, H.; Chen, M.; Sun, Y.; Xu, L.; Li, F.; Han, J. Machine Learning-Assisted Pattern Recognition of Amyloid Beta Aggregates with Fluorescent Conjugated Polymers and Graphite Oxide Electrostatic Complexes. *Anal. Chem.* **2022**, *94*, 2757–2763. [[CrossRef](#)]
77. Wang, H.; Zhou, L.; Qin, J.; Chen, J.; Stewart, C.; Sun, Y.; Huang, H.; Xu, L.; Li, L.; Han, J.; et al. One-Component Multichannel Sensor Array for Rapid Identification of Bacteria. *Anal. Chem.* **2022**, *94*, 10291–10298. [[CrossRef](#)]
78. Yan, P.; Zheng, X.; Liu, S.; Dong, Y.; Fu, T.; Tian, Z.; Wu, Y. Colorimetric Sensor Array for Identification of Proteins and Classification of Metabolic Profiles under Various Osmolyte Conditions. *ACS Sens.* **2023**, *8*, 133–140. [[CrossRef](#)]
79. Izenman, A.J. Linear Discriminant Analysis. In *Modern Multivariate Statistical Techniques: Regression, Classification, and Manifold Learning*; Springer: New York, NY, USA, 2008; pp. 237–280. [[CrossRef](#)]
80. Wold, S.; Esbensen, K.; Geladi, P. Principal component analysis. *Chemom. Intell. Lab. Syst.* **1987**, *2*, 37–52. [[CrossRef](#)]
81. Bridges, C.C. Hierarchical Cluster Analysis. *Psychol. Rep.* **1966**, *18*, 851–854. [[CrossRef](#)]
82. Izenman, A.J. *Modern Multivariate Statistical Techniques: Regression, Classification, and Manifold Learning*; Springer: New York, NY, USA, 2008; pp. 1–731. [[CrossRef](#)]
83. Jolliffe, I.T.; Cadima, J. Principal component analysis: A review and recent developments. *Philos. Trans. R. Soc. A-Math. Phys. Eng. Sci.* **2016**, *374*, 20150202. [[CrossRef](#)]
84. Frades, I.; Matthiesen, R. Overview on Techniques in Cluster Analysis. In *Bioinformatics Methods in Clinical Research*; Matthiesen, R., Ed.; Humana Press: Totowa, NJ, USA, 2010; Volume 593, pp. 81–107.
85. Mitchell, L.; New, E.J.; Mahon, C.S. Macromolecular Optical Sensor Arrays. *ACS Appl. Polym. Mater.* **2021**, *3*, 506–530. [[CrossRef](#)]
86. Yang, X.; Yang, M.; Pang, B.; Vara, M.; Xia, Y. Gold Nanomaterials at Work in Biomedicine. *Chem. Rev.* **2015**, *115*, 10410–10488. [[CrossRef](#)]
87. Jiang, Y.; Shi, M.L.; Liu, Y.; Wan, S.; Cui, C.; Zhang, L.Q.; Tan, W.H. Aptamer/AuNP Biosensor for Colorimetric Profiling of Exosomal Proteins. *Angew. Chem.-Int. Ed.* **2017**, *56*, 11916–11920. [[CrossRef](#)]
88. Nejati, K.; Dadashpour, M.; Gharibi, T.; Mellatyar, H.; Akbarzadeh, A. Biomedical Applications of Functionalized Gold Nanoparticles: A Review. *J. Clust. Sci.* **2022**, *33*, 1–16. [[CrossRef](#)]
89. Miranda, O.R.; Li, X.; Garcia-Gonzalez, L.; Zhu, Z.J.; Yan, B.; Bunz, U.H.; Rotello, V.M. Colorimetric bacteria sensing using a supramolecular enzyme-nanoparticle biosensor. *J. Am. Chem. Soc.* **2011**, *133*, 9650–9653. [[CrossRef](#)]
90. Bajaj, A.; Miranda, O.R.; Kim, I.B.; Phillips, R.L.; Jerry, D.J.; Bunz, U.H.; Rotello, V.M. Detection and differentiation of normal, cancerous, and metastatic cells using nanoparticle-polymer sensor arrays. *Proc. Natl. Acad. Sci. USA* **2009**, *106*, 10912–10916. [[CrossRef](#)]
91. Bajaj, A.; Rana, S.; Miranda, O.R.; Yawe, J.C.; Jerry, D.J.; Bunz, U.H.F.; Rotello, V.M. Cell surface-based differentiation of cell types and cancer states using a gold nanoparticle-GFP based sensing array. *Chem. Sci.* **2010**, *1*, 134. [[CrossRef](#)]
92. Le, N.D.B.; Yesilbag Tonga, G.; Mout, R.; Kim, S.T.; Wille, M.E.; Rana, S.; Dunphy, K.A.; Jerry, D.J.; Yazdani, M.; Ramanathan, R.; et al. Cancer Cell Discrimination Using Host-Guest “Doubled” Arrays. *J. Am. Chem. Soc.* **2017**, *139*, 8008–8012. [[CrossRef](#)]
93. Yang, J.E.; Lu, Y.X.; Ao, L.; Wang, F.Y.; Jing, W.J.; Zhang, S.C.; Liu, Y.Y. Colorimetric sensor array for proteins discrimination based on the tunable peroxidase-like activity of AuNPs-DNA conjugates. *Sens. Actuators B-Chem.* **2017**, *245*, 66–73. [[CrossRef](#)]
94. Wang, F.Y.; Zhang, X.; Lu, Y.X.; Yang, J.O.; Jing, W.J.; Zhang, S.C.; Liu, Y.Y. Continuously evolving ‘chemical tongue’ biosensor for detecting proteins. *Talanta* **2017**, *165*, 182–187. [[CrossRef](#)]
95. Lin, X.; Hai, X.; Wang, N.; Chen, X.W.; Wang, J.H. Dual-signal model array sensor based on GQDs/AuNPs system for sensitive protein discrimination. *Anal. Chim. Acta* **2017**, *992*, 105–111. [[CrossRef](#)]
96. Mao, J.P.; Lu, Y.X.; Chang, N.; Yang, J.E.; Zhang, S.C.; Liu, Y.Y. Multidimensional colorimetric sensor array for discrimination of proteins. *Biosens. Bioelectron.* **2016**, *86*, 56–61. [[CrossRef](#)]
97. Jiang, M.D.; Gupta, A.; Zhang, X.Z.; Chattopadhyay, A.N.; Fedeli, S.; Huang, R.; Yang, J.; Rotello, V.M. Identification of Proteins Using Supramolecular Gold Nanoparticle-Dye Sensor Arrays. *Anal. Sens.* **2023**, *3*, e202200080. [[CrossRef](#)]
98. Bian, M.M.; Xu, M.; Yuan, Y.L.; Nie, J.F. Colorimetric Array Sensor for Discrimination of Multiple Heavy Metal Ions Based on Different Lengths of DNA-AuNPs. *Chin. J. Anal. Chem.* **2020**, *48*, 863–870. [[CrossRef](#)]
99. Li, L.; CiRen, D.; Chen, Z.B. Gold Nanoparticles-Based Dual-Channel Colorimetric Array Sensors for Discrimination of Metal Ions. *ACS Appl. Nano Mater.* **2022**, *5*, 18270–18275. [[CrossRef](#)]
100. Liu, Q.; Yeh, Y.C.; Rana, S.; Jiang, Y.; Guo, L.; Rotello, V.M. Differentiation of cancer cell type and phenotype using quantum dot-gold nanoparticle sensor arrays. *Cancer Lett.* **2013**, *334*, 196–201. [[CrossRef](#)]
101. Wei, X.C.; Chen, Z.B.; Tan, L.L.; Lou, T.H.; Zhao, Y. DNA-Catalytically Active Gold Nanoparticle Conjugates-Based Colorimetric Multidimensional Sensor Array for Protein Discrimination. *Anal. Chem.* **2017**, *89*, 556–559. [[CrossRef](#)]

102. Xu, Y.; Qian, C.; Yu, Y.; Yang, S.J.; Shi, F.F.; Gao, X.; Liu, Y.H.; Huang, H.; Stewart, C.; Li, F.; et al. Machine Learning-Assisted Nanoenzyme/Bioenzyme Dual-Coupled Array for Rapid Detection of Amyloids. *Anal. Chem.* **2023**, *95*, 4605–4611. [[CrossRef](#)]
103. Abbasi-Moayed, S.; Orouji, A.; Hormozi-Nezhad, M.R. Multiplex Detection of Biogenic Amines for Meat Freshness Monitoring Using Nanoplasmonic Colorimetric Sensor Array. *Biosensors* **2023**, *13*, 803. [[CrossRef](#)]
104. Chen, X.L.; Liang, Y. Colorimetric sensing strategy for multiplexed detection of proteins based on three DNA-gold nanoparticle conjugates sensors. *Sens. Actuators B-Chem.* **2021**, *329*, 129202. [[CrossRef](#)]
105. Wong, S.F.; Khor, S.M. Differential colorimetric nanobiosensor array as bioelectronic tongue for discrimination and quantitation of multiple foodborne carcinogens. *Food Chem.* **2021**, *357*, 129801. [[CrossRef](#)]
106. Li, Y.N.; Liu, Q.Y.; Chen, Z.B. A colorimetric sensor array for detection and discrimination of antioxidants based on Ag nanoshell deposition on gold nanoparticle surfaces. *Analyst* **2019**, *144*, 6276–6282. [[CrossRef](#)]
107. Yang, J.Y.; Yang, T.; Wang, X.Y.; Wang, Y.T.; Liu, M.X.; Chen, M.L.; Yu, Y.L.; Wang, J.H. A Novel Three-Dimensional Nanosensing Array for the Discrimination of Sulfur-Containing Species and Sulfur Bacteria. *Anal. Chem.* **2019**, *91*, 6012–6018. [[CrossRef](#)]
108. Li, D.Y.; Dong, Y.H.; Li, B.Y.; Wu, Y.Y.; Wang, K.; Zhang, S.C. Colorimetric sensor array with unmodified noble metal nanoparticles for naked-eye detection of proteins and bacteria. *Analyst* **2015**, *140*, 7672–7677. [[CrossRef](#)]
109. Jia, F.; Huang, J.; Wei, W.; Chen, Z.; Zhou, Q. Visual sensing of flavonoids based on varying degrees of gold nanoparticle aggregation via linear discriminant analysis. *Sens. Actuators B Chem.* **2021**, *348*, 130685. [[CrossRef](#)]
110. Leng, Y.; Cheng, J.; Liu, C.; Wang, D.; Lu, Z.; Ma, C.; Zhang, M.; Dong, Y.; Xing, X.; Yao, L.; et al. A rapid reduction of Au(I→0) strategy for the colorimetric detection and discrimination of proteins. *Microchim. Acta* **2021**, *188*, 249. [[CrossRef](#)]
111. Qiang, H.; Wei, X.; Liu, Q.; Chen, Z. Iodide-Responsive Cu–Au Nanoparticle-Based Colorimetric Sensor Array for Protein Discrimination. *ACS Sustain. Chem. Eng.* **2018**, *6*, 15720–15726. [[CrossRef](#)]
112. Xi, H.; He, W.; Liu, Q.; Chen, Z. Protein Discrimination Using a Colorimetric Sensor Array Based on Gold Nanoparticle Aggregation Induced by Cationic Polymer. *ACS Sustain. Chem. Eng.* **2018**, *6*, 10751–10757. [[CrossRef](#)]
113. Das Saha, N.; Sasmal, R.; Meethal, S.K.; Vats, S.; Gopinathan, P.V.; Jash, O.; Manjithaya, R.; Gagey-Eilstein, N.; Agasti, S.S. Multichannel DNA Sensor Array Fingerprints Cell States and Identifies Pharmacological Effectors of Catabolic Processes. *ACS Sens.* **2019**, *4*, 3124–3132. [[CrossRef](#)]
114. Mayilo, S.; Kloster, M.A.; Wunderlich, M.; Lutich, A.; Klar, T.A.; Nichtl, A.; Kürzinger, K.; Stefani, F.D.; Feldmann, J. Long-Range Fluorescence Quenching by Gold Nanoparticles in a Sandwich Immunoassay for Cardiac Troponin T. *Nano Lett.* **2009**, *9*, 4558–4563. [[CrossRef](#)]
115. Hung, S.Y.; Shih, Y.C.; Tseng, W.L. Tween 20-stabilized gold nanoparticles combined with adenosine triphosphate-BODIPY conjugates for the fluorescence detection of adenosine with more than 1000-fold selectivity. *Anal. Chim. Acta* **2015**, *857*, 64–70. [[CrossRef](#)]
116. Lu, S.S.; Wang, S.; Chen, C.X.; Sun, J.; Yang, X.R. Enzyme-free aptamer/AuNPs-based fluorometric and colorimetric dual-mode detection for ATP. *Sens. Actuators B-Chem.* **2018**, *265*, 67–74. [[CrossRef](#)]
117. Lv, L.; Jin, Y.D.; Kang, X.J.; Zhao, Y.Y.; Cui, C.B.; Guo, Z.J. PVP-coated gold nanoparticles for the selective determination of ochratoxin A via quenching fluorescence of the free aptamer. *Food Chem.* **2018**, *249*, 45–50. [[CrossRef](#)]
118. Saad, S.M.; Abdullah, J.; Abd Rashid, S.; Fen, Y.W.; Salam, F.; Yih, L.H. A fluorescence quenching based gene assay for *Escherichia coli* O157:H7 using graphene quantum dots and gold nanoparticles. *Microchim. Acta* **2019**, *186*, 804. [[CrossRef](#)]
119. Chen, Y.S.; Chen, Z.W.; Yuan, Y.W.; Chen, K.C.; Liu, C.P. Fluorescence Quenchers Manipulate the Peroxidase-like Activity of Gold-Based Nanomaterials. *ACS Omega* **2020**, *5*, 24487–24494. [[CrossRef](#)]
120. Saad, S.M.; Abdullah, J.; Abd Rashid, S.; Fen, Y.W.; Salam, F.; Yih, L.H. A carbon dots based fluorescence sensing for the determination of *Escherichia coli* O157:H7. *Measurement* **2020**, *160*, 107845. [[CrossRef](#)]
121. Jiang, W.; Wang, Z.; Beier, R.C.; Jiang, H.; Wu, Y.; Shen, J. Simultaneous determination of 13 fluoroquinolone and 22 sulfonamide residues in milk by a dual-colorimetric enzyme-linked immunosorbent assay. *Anal. Chem.* **2013**, *85*, 1995–1999. [[CrossRef](#)]
122. Bajaj, A.; Miranda, O.R.; Phillips, R.; Kim, I.-B.; Jerry, D.J.; Bunz, U.H.F.; Rotello, V.M. Array-Based Sensing of Normal, Cancerous, and Metastatic Cells Using Conjugated Fluorescent Polymers. *J. Am. Chem. Soc.* **2010**, *132*, 1018–1022. [[CrossRef](#)]
123. Kumar, V.V.; Anthony, S.P. Highly selective colorimetric sensing of Hg²⁺ ions by label free AuNPs in aqueous medium across wide pH range. *Sens. Actuators B-Chem.* **2016**, *225*, 413–419. [[CrossRef](#)]
124. Liu, X.H.; Wang, Y.; Chen, P.; McCadden, A.; Palaniappan, A.; Zhang, J.L.; Liedberg, B. Peptide Functionalized Gold Nanoparticles with Optimized Particle Size and Concentration for Colorimetric Assay Development: Detection of Cardiac Troponin I. *ACS Sens.* **2016**, *1*, 1416–1422. [[CrossRef](#)]
125. Yang, J.J.; Feng, L.J.; Liu, J.; Li, S.; Li, N.; Zhang, X.F. DNA-mediated charge neutralization of AuNPs for colorimetric sensing of Hg²⁺ in environmental waters and cosmetics. *Sens. Actuators B-Chem.* **2024**, *398*, 134697. [[CrossRef](#)]
126. Lu, Y.; Liu, Y.; Zhang, S.; Wang, S.; Zhang, S.; Zhang, X. Aptamer-based plasmonic sensor array for discrimination of proteins and cells with the naked eye. *Anal. Chem.* **2013**, *85*, 6571–6574. [[CrossRef](#)]
127. Sun, W.; Lu, Y.; Mao, J.; Chang, N.; Yang, J.; Liu, Y. Multidimensional sensor for pattern recognition of proteins based on DNA-gold nanoparticles conjugates. *Anal. Chem.* **2015**, *87*, 3354–3359. [[CrossRef](#)]
128. Wei, X.; Wang, Y.; Zhao, Y.; Chen, Z. Colorimetric sensor array for protein discrimination based on different DNA chain length-dependent gold nanoparticles aggregation. *Biosens. Bioelectron.* **2017**, *97*, 332–337. [[CrossRef](#)]

129. Yang, X.; Li, J.; Pei, H.; Zhao, Y.; Zuo, X.; Fan, C.; Huang, Q. DNA-gold nanoparticle conjugates-based nanoplasmonic probe for specific differentiation of cell types. *Anal. Chem.* **2014**, *86*, 3227–3231. [[CrossRef](#)]
130. Gao, X.; Li, M.; Zhao, M.; Wang, X.; Wang, S.; Liu, Y. Metabolism-Triggered Colorimetric Sensor Array for Fingerprinting and Antibiotic Susceptibility Testing of Bacteria. *Anal. Chem.* **2022**, *94*, 6957–6966. [[CrossRef](#)]
131. Tang, Z.; Chen, F.; Wang, D.; Xiong, D.; Yan, S.; Liu, S.; Tang, H. Fabrication of avidin-stabilized gold nanoclusters with dual emissions and their application in biosensing. *J. Nanobiotechnology* **2022**, *20*, 306. [[CrossRef](#)]
132. Biswas, A.; Banerjee, S.; Gart, E.V.; Nagaraja, A.T.; McShane, M.J. Gold Nanocluster Containing Polymeric Microcapsules for Intracellular Ratiometric Fluorescence Biosensing. *ACS Omega* **2017**, *2*, 2499–2506. [[CrossRef](#)]
133. Niazi, S.; Khan, I.M.; Akhtar, W.; ul Haq, F.; Pasha, I.; Khan, M.K.I.; Mohsin, A.; Ahmad, S.; Zhang, Y.; Wang, Z. Aptamer functionalized gold nanoclusters as an emerging nanoprobe in biosensing, diagnostic, catalysis and bioimaging. *Talanta* **2024**, *268*, 125270. [[CrossRef](#)]
134. Zhang, Y.; Zhang, C.; Xu, C.; Wang, X.; Liu, C.; Waterhouse, G.I.N.; Wang, Y.; Yin, H. Ultrasmall Au nanoclusters for biomedical and biosensing applications: A mini-review. *Talanta* **2019**, *200*, 432–442. [[CrossRef](#)]
135. Gan, Z.B.; Lin, Y.J.; Luo, L.; Han, G.M.; Liu, W.; Liu, Z.J.; Yao, C.H.; Weng, L.H.; Liao, L.W.; Chen, J.S.; et al. Fluorescent Gold Nanoclusters with Interlocked Staples and a Fully Thiolate-Bound Kernel. *Angew. Chem.-Int. Ed.* **2016**, *55*, 11567–11571. [[CrossRef](#)] [[PubMed](#)]
136. Guo, Y.H.; Amunyela, H.; Cheng, Y.L.; Xie, Y.F.; Yu, H.; Yao, W.R.; Li, H.W.; Qian, H. Natural protein-templated fluorescent gold nanoclusters: Syntheses and applications. *Food Chem.* **2021**, *335*, 127657. [[CrossRef](#)]
137. Sonia; Komal; Kukreti, S.; Kaushik, M. Gold nanoclusters: An ultrasmall platform for multifaceted applications. *Talanta* **2021**, *234*, 122623. [[CrossRef](#)]
138. Sun, Y.F.; Zhou, Z.P.; Shu, T.; Qian, L.S.; Su, L.; Zhang, X.J. Multicolor Luminescent Gold Nanoclusters: From Structure to Biosensing and Bioimaging. *Prog. Chem.* **2021**, *33*, 179–187. [[CrossRef](#)]
139. Chen, S.Q.; Li, S.S.; Wang, Y.L.; Chen, Z.H.; Wang, H.; Zhang, X.D. Gold Nanoclusters for Tumor Diagnosis and Treatment. *Adv. Nanobiomed Res.* **2023**, *3*, 2300082. [[CrossRef](#)]
140. Ivanova, N.K.; Karpushkin, E.A.; Lopatina, L.I.; Sergeev, V.G. DNA as a template for synthesis of fluorescent gold nanoclusters. *Mendeleev Commun.* **2023**, *33*, 346–348. [[CrossRef](#)]
141. Liu, Z.Y.; Luo, L.S.; Jin, R.C. Visible to NIR-II Photoluminescence of Atomically Precise Gold Nanoclusters. *Adv. Mater.* **2023**, *36*, e2309073. [[CrossRef](#)] [[PubMed](#)]
142. Zhou, S.C.; Gustavsson, L.; Beaune, G.; Chandra, S.; Niskanen, J.; Ruokolainen, J.; Timonen, J.V.I.; Ikkala, O.; Peng, B.; Ras, R.H.A. pH-Responsive Near-Infrared Emitting Gold Nanoclusters. *Angew. Chem.-Int. Ed.* **2023**, *62*, e202312679. [[CrossRef](#)]
143. Sun, M.; Wu, L.; Ren, H.; Chen, X.; Ouyang, J.; Na, N. Radical-Mediated Spin-Transfer on Gold Nanoclusters Driven an Unexpected Luminescence for Protein Discrimination. *Anal. Chem.* **2017**, *89*, 11183–11188. [[CrossRef](#)]
144. Xu, S.; Gao, T.; Feng, X.; Fan, X.; Liu, G.; Mao, Y.; Yu, X.; Lin, J.; Luo, X. Near infrared fluorescent dual ligand functionalized Au NCs based multidimensional sensor array for pattern recognition of multiple proteins and serum discrimination. *Biosens. Bioelectron.* **2017**, *97*, 203–207. [[CrossRef](#)]
145. Xu, S.; Li, W.; Zhao, X.; Wu, T.; Cui, Y.; Fan, X.; Wang, W.; Luo, X. Ultrahighly Efficient and Stable Fluorescent Gold Nanoclusters Coated with Screened Peptides of Unique Sequences for Effective Protein and Serum Discrimination. *Anal. Chem.* **2019**, *91*, 13947–13952. [[CrossRef](#)] [[PubMed](#)]
146. Wu, Y.; Wang, B.; Wang, K.; Yan, P. Identification of proteins and bacteria based on a metal ion–gold nanocluster sensor array. *Anal. Methods* **2018**, *10*, 3939–3944. [[CrossRef](#)]
147. Lu, H.; Lu, Q.; Sun, H.; Wang, Z.; Shi, X.; Ding, Y.; Ran, X.; Pei, J.; Pan, Y.; Zhang, Q. ROS-Responsive Fluorescent Sensor Array for Precise Diagnosis of Cancer via pH-Controlled Multicolor Gold Nanoclusters. *ACS Appl. Mater. Interfaces* **2023**, *15*, 38381–38390. [[CrossRef](#)] [[PubMed](#)]
148. Xiao, Y.; Cheng, P.; Zhu, X.; Xu, M.; Liu, M.; Li, H.; Zhang, Y.; Yao, S. Antimicrobial Agent Functional Gold Nanocluster-Mediated Multichannel Sensor Array for Bacteria Sensing. *Langmuir* **2024**, *40*, 2369–2376. [[CrossRef](#)]
149. Li, X.; Kong, H.; Mout, R.; Saha, K.; Moyano, D.F.; Robinson, S.M.; Rana, S.; Zhang, X.; Riley, M.A.; Rotello, V.M. Rapid Identification of Bacterial Biofilms and Biofilm Wound Models Using a Multichannel Nanosensor. *ACS Nano* **2014**, *8*, 12014–12019. [[CrossRef](#)] [[PubMed](#)]
150. Tomita, S.; Matsuda, A.; Nishinami, S.; Kurita, R.; Shiraki, K. One-Step Identification of Antibody Degradation Pathways Using Fluorescence Signatures Generated by Cross-Reactive DNA-Based Arrays. *Anal. Chem.* **2017**, *89*, 7818–7822. [[CrossRef](#)] [[PubMed](#)]
151. Xu, L.Q.; Wang, L.; Zhang, B.; Lim, C.H.; Chen, Y.; Neoh, K.-G.; Kang, E.-T.; Fu, G.D. Functionalization of reduced graphene oxide nanosheets via stacking interactions with the fluorescent and water-soluble perylene bisimide-containing polymers. *Polymer* **2011**, *52*, 2376–2383. [[CrossRef](#)]
152. Suguna, S.; David, C.I.; Prabhu, J.; Nandhakumar, R. Functionalized graphene oxide materials for the fluorometric sensing of various analytes: A mini review. *Mater. Adv.* **2021**, *2*, 6197–6212. [[CrossRef](#)]
153. Tao, Y.; Auguste, D.T. Array-based identification of triple-negative breast cancer cells using fluorescent nanodot-graphene oxide complexes. *Biosens. Bioelectron.* **2016**, *81*, 431–437. [[CrossRef](#)]
154. Hizir, M.S.; Robertson, N.M.; Balcioglu, M.; Alp, E.; Rana, M.; Yigit, M.V. Universal sensor array for highly selective system identification using two-dimensional nanoparticles. *Chem. Sci.* **2017**, *8*, 5735–5745. [[CrossRef](#)]

155. Park, J.S.; Goo, N.I.; Kim, D.E. Mechanism of DNA Adsorption and Desorption on Graphene Oxide. *Langmuir* **2014**, *30*, 12587–12595. [[CrossRef](#)]
156. Lu, C.; Huang, P.J.J.; Liu, B.W.; Ying, Y.B.; Liu, J.W. Comparison of Graphene Oxide and Reduced Graphene Oxide for DNA Adsorption and Sensing. *Langmuir* **2016**, *32*, 10776–10783. [[CrossRef](#)]
157. Lu, C.; Liu, Y.B.; Ying, Y.B.; Liu, J.W. Comparison of MoS₂, WS₂, and Graphene Oxide for DNA Adsorption and Sensing. *Langmuir* **2017**, *33*, 630–637. [[CrossRef](#)]
158. Lu, Z.J.; Wang, P.; Xiong, W.W.; Qi, B.P.; Shi, R.J.; Xiang, D.S.; Zhai, K. Simultaneous detection of mercury (II), lead (II) and silver (I) based on fluorescently labelled aptamer probes and graphene oxide. *Environ. Technol.* **2021**, *42*, 3065–3072. [[CrossRef](#)]
159. Morales-Narvaez, E.; Merkoci, A. Graphene Oxide as an Optical Biosensing Platform: A Progress Report. *Adv. Mater.* **2019**, *31*, e1805043. [[CrossRef](#)]
160. Yu, W.; Sisi, L.; Haiyan, Y.; Jie, L. Progress in the functional modification of graphene/graphene oxide: A review. *RSC Adv.* **2020**, *10*, 15328–15345. [[CrossRef](#)]
161. Behera, P.; De, M. Nano-Graphene Oxide Based Multichannel Sensor Arrays towards Sensing of Protein Mixtures. *Chem.-Asian J.* **2019**, *14*, 553–560. [[CrossRef](#)]
162. Zhu, Q.Y.; Zhang, F.R.; Du, Y.; Zhang, X.X.; Lu, J.Y.; Yao, Q.F.; Huang, W.T.; Ding, X.Z.; Xia, L.Q. Graphene-Based Steganographically Aptasensing System for Information Computing, Encryption and Hiding, Fluorescence Sensing and in Vivo Imaging of Fish Pathogens. *ACS Appl. Mater. Interfaces* **2019**, *11*, 8904–8914. [[CrossRef](#)]
163. Tomita, S.; Ishihara, S.; Kurita, R. A Multi-Fluorescent DNA/Graphene Oxide Conjugate Sensor for Signature-Based Protein Discrimination. *Sensors* **2017**, *17*, 2194. [[CrossRef](#)]
164. Lin, M.; Li, W.S.; Wang, Y.L.; Yang, X.H.; Wang, K.M.; Wang, Q.; Wang, P.; Chang, Y.J.; Tan, Y.Y. Discrimination of hemoglobins with subtle differences using an aptamer based sensing array. *Chem. Commun.* **2015**, *51*, 8304–8306. [[CrossRef](#)]
165. Fu, M.Q.; Wang, X.C.; Dou, W.T.; Chen, G.R.; James, T.D.; Zhou, D.M.; He, X.P. Supramolecular fluorogenic peptide sensor array based on graphene oxide for the differential sensing of ebola virus. *Chem. Commun.* **2020**, *56*, 5735–5738. [[CrossRef](#)] [[PubMed](#)]
166. Nandu, N.; Smith, C.W.; Uyar, T.B.; Chen, Y.S.; Kachwala, M.J.; He, M.H.; Yigit, M.V. Machine-Learning Single-Stranded DNA Nanoparticles for Bacterial Analysis. *ACS Applied. Nano Mater.* **2020**, *3*, 11709–11714. [[CrossRef](#)] [[PubMed](#)]
167. Shen, J.; Hu, R.; Zhou, T.; Wang, Z.; Zhang, Y.; Li, S.; Gui, C.; Jiang, M.; Qin, A.; Tang, B.Z. Fluorescent Sensor Array for Highly Efficient Microbial Lysate Identification through Competitive Interactions. *ACS Sens.* **2018**, *3*, 2218–2222. [[CrossRef](#)]
168. Martynenko, I.V.; Litvin, A.P.; Purcell-Milton, F.; Baranov, A.V.; Fedorov, A.V.; Gun'ko, Y.K. Application of semiconductor quantum dots in bioimaging and biosensing. *J. Mater. Chem. B* **2017**, *5*, 6701–6727. [[CrossRef](#)]
169. Freire, R.M.; Le, N.D.B.; Jiang, Z.W.; Kim, C.S.; Rotello, V.M.; Fehine, P.B.A. NH₂-rich Carbon Quantum Dots: A protein-responsive probe for detection and identification. *Sens. Actuators B-Chem.* **2018**, *255*, 2725–2732. [[CrossRef](#)]
170. Zheng, L.B.; Qi, P.; Zhang, D. Identification of bacteria by a fluorescence sensor array based on three kinds of receptors functionalized carbon dots. *Sens. Actuators B-Chem.* **2019**, *286*, 206–213. [[CrossRef](#)]
171. Wang, M.; Ye, H.; You, L.; Chen, X. A Supramolecular Sensor Array Using Lanthanide-Doped Nanoparticles for Sensitive Detection of Glyphosate and Proteins. *ACS Appl. Mater. Interfaces* **2016**, *8*, 574–581. [[CrossRef](#)]
172. Wu, Y.; Tan, Y.; Wu, J.; Chen, S.; Chen, Y.Z.; Zhou, X.; Jiang, Y.; Tan, C. Fluorescence array-based sensing of metal ions using conjugated polyelectrolytes. *ACS Appl. Mater. Interfaces* **2015**, *7*, 6882–6888. [[CrossRef](#)]
173. Wu, P.; Miao, L.N.; Wang, H.F.; Shao, X.G.; Yan, X.P. A multidimensional sensing device for the discrimination of proteins based on manganese-doped ZnS quantum dots. *Angew. Chem. Int. Ed. Engl.* **2011**, *50*, 8118–8121. [[CrossRef](#)]
174. Wang, K.; Dong, Y.; Li, B.; Li, D.; Zhang, S.; Wu, Y. Differentiation of proteins and cancer cells using metal oxide and metal nanoparticles-quantum dots sensor array. *Sens. Actuators B Chem.* **2017**, *250*, 69–75. [[CrossRef](#)]
175. Chen, S.; Wei, L.; Chen, X.W.; Wang, J.H. Suspension Array of Ionic Liquid or Ionic Liquid-Quantum Dots Conjugates for the Discrimination of Proteins and Bacteria. *Anal. Chem.* **2015**, *87*, 10902–10909. [[CrossRef](#)]
176. Lu, Z.; Lu, N.; Xiao, Y.; Zhang, Y.; Tang, Z.; Zhang, M. Metal-Nanoparticle-Supported Nanozyme-Based Colorimetric Sensor Array for Precise Identification of Proteins and Oral Bacteria. *ACS Appl. Mater. Interfaces* **2022**, *14*, 11156–11166. [[CrossRef](#)]
177. Zhang, L.; Qi, Z.; Yang, Y.; Lu, N.; Tang, Z. Enhanced “Electronic Tongue” for Dental Bacterial Discrimination and Elimination Based on a DNA-Encoded Nanozyme Sensor Array. *ACS Appl. Mater. Interfaces* **2024**, *16*, 11228–11238. [[CrossRef](#)]
178. Chen, H.; Guo, S.; Zhuang, Z.; Ouyang, S.; Lin, P.; Zheng, Z.; You, Y.; Zhou, X.; Li, Y.; Lu, J.; et al. Intelligent Identification of Cerebrospinal Fluid for the Diagnosis of Parkinson's Disease. *Anal. Chem.* **2024**, *96*, 2534–2542. [[CrossRef](#)]
179. Yang, J.; Lu, S.; Chen, B.; Hu, F.; Li, C.; Guo, C. Machine learning-assisted optical nano-sensor arrays in microorganism analysis. *TrAC Trends Anal. Chem.* **2023**, *159*, 116945. [[CrossRef](#)]
180. Behera, P.; Singh, K.K.; Pandit, S.; Saha, D.; Saini, D.K.; De, M. Machine Learning-Assisted Array-Based Detection of Proteins in Serum Using Functionalized MoS₂ Nanosheets and Green Fluorescent Protein Conjugates. *ACS Appl. Nano Mater.* **2021**, *4*, 3843–3851. [[CrossRef](#)]
181. Yan, P.; Ding, Z.; Li, X.; Dong, Y.; Fu, T.; Wu, Y. Colorimetric Sensor Array Based on Wulff-Type Boronate Functionalized AgNPs at Various pH for Bacteria Identification. *Anal. Chem.* **2019**, *91*, 12134–12137. [[CrossRef](#)]
182. Yang, H.M.; Jie, X.; Wang, L.; Zhang, Y.; Wang, M.; Wei, W.L. An array consisting of glycosylated quantum dots conjugated to MoS₂ nanosheets for fluorometric identification and quantitation of lectins and bacteria. *Microchimica Acta* **2018**, *185*, 512. [[CrossRef](#)]

183. Behera, P.; Kumar Singh, K.; Kumar Saini, D.; De, M. Rapid Discrimination of Bacterial Drug Resistivity by Array-Based Cross-Validation Using 2D MoS₂. *Chem.—A Eur. J.* **2022**, *28*, e202201386. [[CrossRef](#)]
184. He, Y.; He, X.; Liu, X.; Gao, L.; Cui, H. Dynamically tunable chemiluminescence of luminol-functionalized silver nanoparticles and its application to protein sensing arrays. *Anal. Chem.* **2014**, *86*, 12166–12171. [[CrossRef](#)]
185. Pu, F.; Ran, X.; Guan, M.; Huang, Y.; Ren, J.; Qu, X. Biomolecule-templated photochemical synthesis of silver nanoparticles: Multiple readouts of localized surface plasmon resonance for pattern recognition. *Nano Res.* **2017**, *11*, 3213–3221. [[CrossRef](#)]
186. Ran, X.; Pu, F.; Ren, J.; Qu, X. A CuS-based chemical tongue chip for pattern recognition of proteins and antibiotic-resistant bacteria. *Chem. Commun.* **2015**, *51*, 2675–2678. [[CrossRef](#)] [[PubMed](#)]
187. Wan, Y.; Sun, Y.; Qi, P.; Wang, P.; Zhang, D. Quaternized magnetic nanoparticles-fluorescent polymer system for detection and identification of bacteria. *Biosens. Bioelectron.* **2014**, *55*, 289–293. [[CrossRef](#)] [[PubMed](#)]
188. Sabela, M.; Balme, S.; Bechelany, M.; Janot, J.M.; Bisetty, K. A Review of Gold and Silver Nanoparticle-Based Colorimetric Sensing Assays. *Adv. Eng. Mater.* **2017**, *19*, 1700270. [[CrossRef](#)]
189. Geng, Y.; Peveler, W.J.; Rotello, V.M. Array-based “Chemical Nose” Sensing in Diagnostics and Drug Discovery. *Angew. Chem.-Int. Ed.* **2019**, *58*, 5190–5200. [[CrossRef](#)]
190. Medrano-Lopez, J.A.; Villalpando, I.; Salazar, M.I.; Torres-Torres, C. Hierarchical Nanobiosensors at the End of the SARS-CoV-2 Pandemic. *Biosensors* **2024**, *14*, 108. [[CrossRef](#)]
191. Behera, P.; De, M.M. Surface-Engineered Nanomaterials for Optical Array Based Sensing. *Chempluschem* **2023**, e202300610. [[CrossRef](#)]

Disclaimer/Publisher’s Note: The statements, opinions and data contained in all publications are solely those of the individual author(s) and contributor(s) and not of MDPI and/or the editor(s). MDPI and/or the editor(s) disclaim responsibility for any injury to people or property resulting from any ideas, methods, instructions or products referred to in the content.